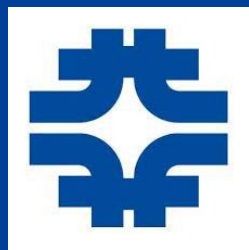
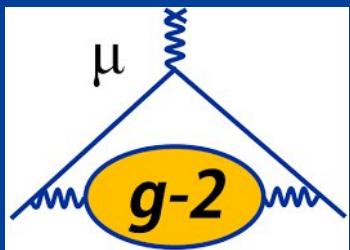


The Fermilab Muon $g-2$ Experiment

Siew Yan Hoh, Yusuke Takeuchi, Jun Kai Ng,
YongHao Zheng, ZeJia Lu, Li Liang, Kim Sing Khaw

MIP 2024 @ Peking University, Beijing.
19-22 April 2024



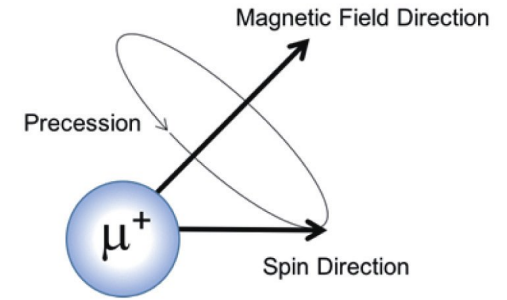
李政道研究所
TSUNG-DAO LEE INSTITUTE



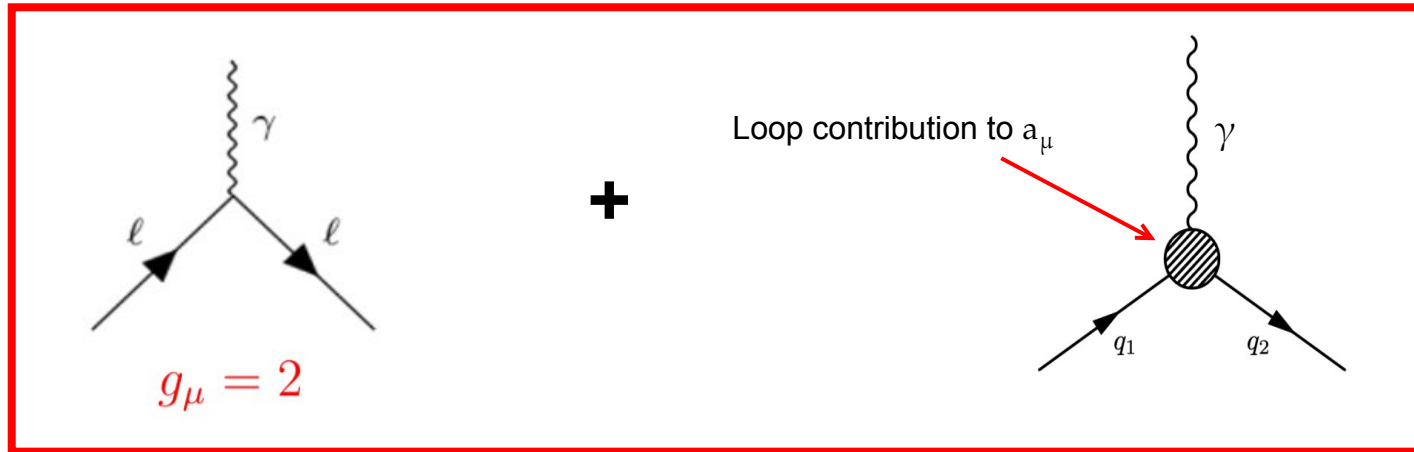
Anomalous Magnetic Moment

- The magnetic moment for the charged muon is given by:

$$\vec{\mu}_\mu = g_\mu \frac{e}{2m_\mu} \vec{s}$$



- Dirac predicts $g_\mu = 2$; additional contribution from quantum effects changes the g-factor values:



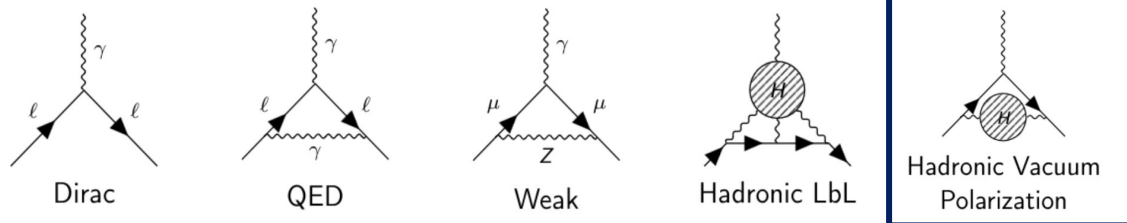
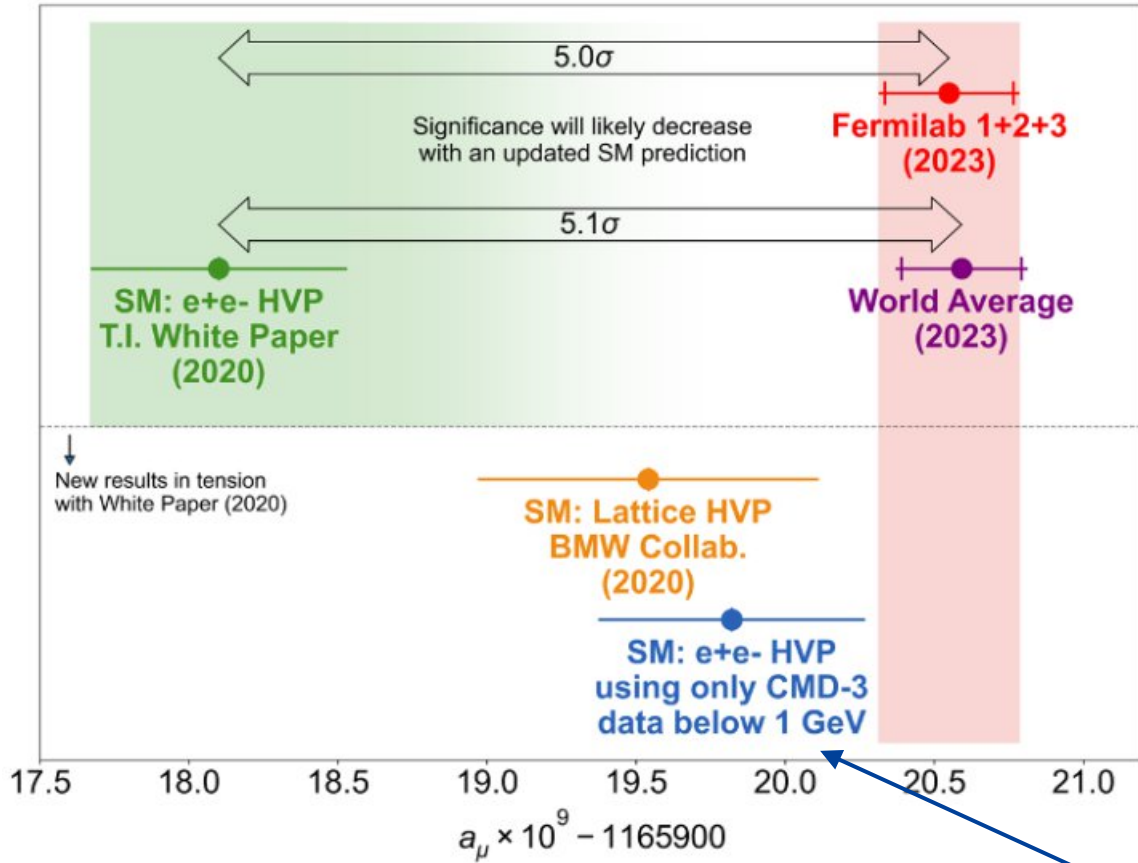
$$g_\mu = 2 + 2 \underbrace{\left(\frac{\alpha}{2\pi} + \mathcal{O}(\alpha^2) \right)}_{\equiv a_\mu}$$

$$a_\mu = \frac{g_\mu - 2}{2} \neq 0$$

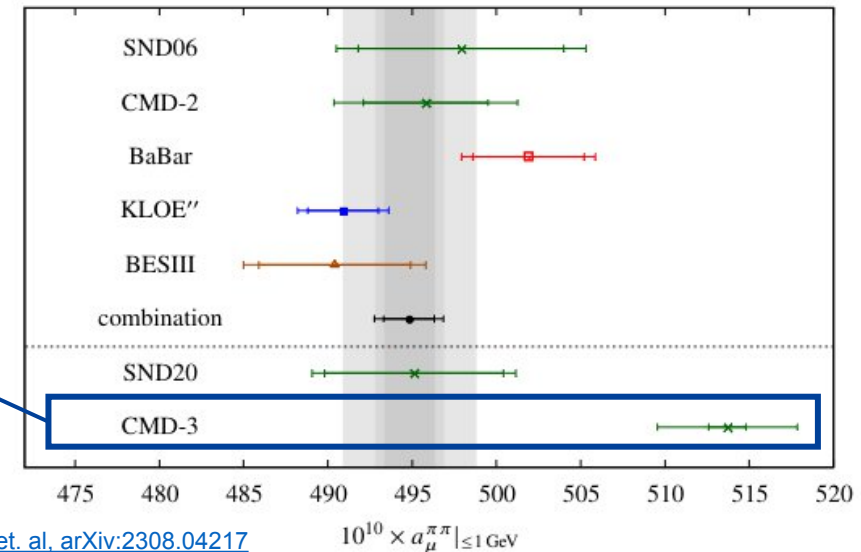
- Quantum effects can be measured via anomalous magnetic moment

- Sensitive to new physics contribution at mass scale: $\frac{\delta a_\mu}{a_\mu} \sim \mathcal{O} \left(\frac{m_\mu}{\Lambda} \right)^2$

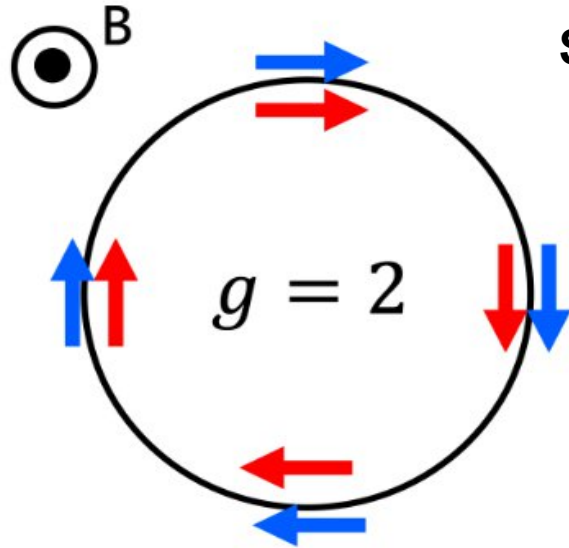
Theoretical Prediction and Measurement



- FNAL result yields 5 σ disagreement with WP (2020).
- However, HVP prediction is different, depending on the methods:
 - Swaps HVP value from BMW into WP (2020) reduces the discrepancy with the experimental value.
 - Result results using e⁺e⁻ data from CMD-3 further reduces the discrepancy.

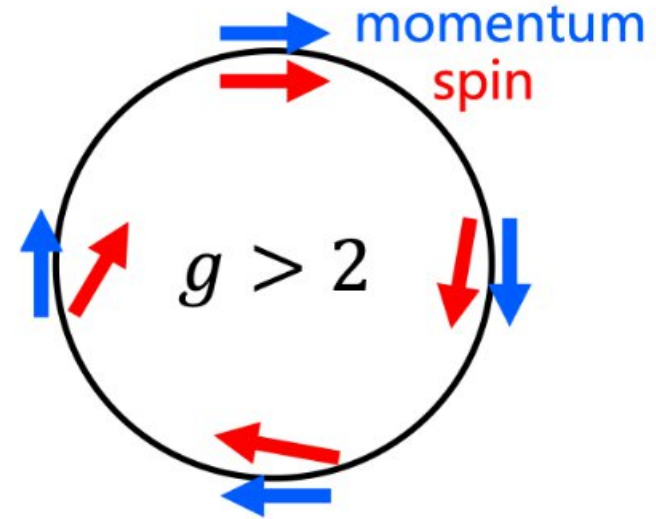


Measuring a_μ In Storage Ring



Stored polarized μ^+ in dipole field

$$a_\mu = \frac{g_\mu - 2}{2}$$



$a_\mu = 0$: spin and momentum precess
at the same rate

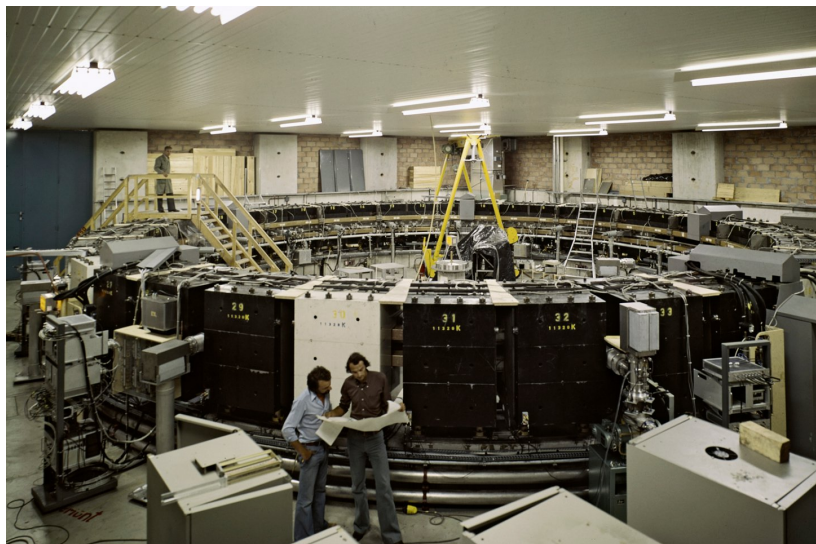
$a_\mu > 0$: spin has precession motion around
the momentum vector

Measuring the difference, **anomalous spin precession frequency** between the spin precession and cyclotron frequencies:

$$\vec{\omega}_a = a_\mu \frac{e}{m_\mu c} \vec{B} \quad \rightarrow \quad a_\mu = \frac{\omega_a}{B} \cdot \frac{m_\mu c}{e}$$

measure ω^a and \mathbf{B} as precisely as possible, $\sim O(200\text{ppb})$

The Storage Rings



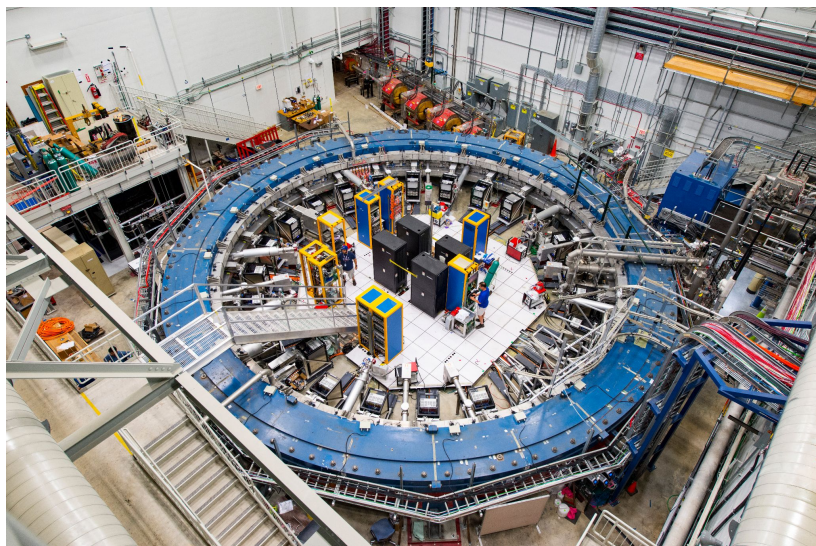
CERN
1960s - 1976
7.3 ppm

COMPLETED

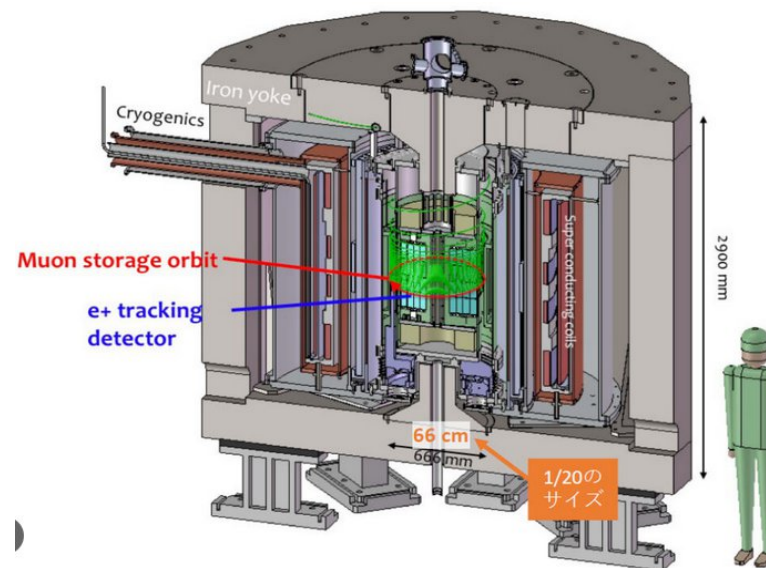
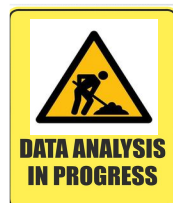


BNL
1990s - 2001
0.54 ppm

COMPLETED



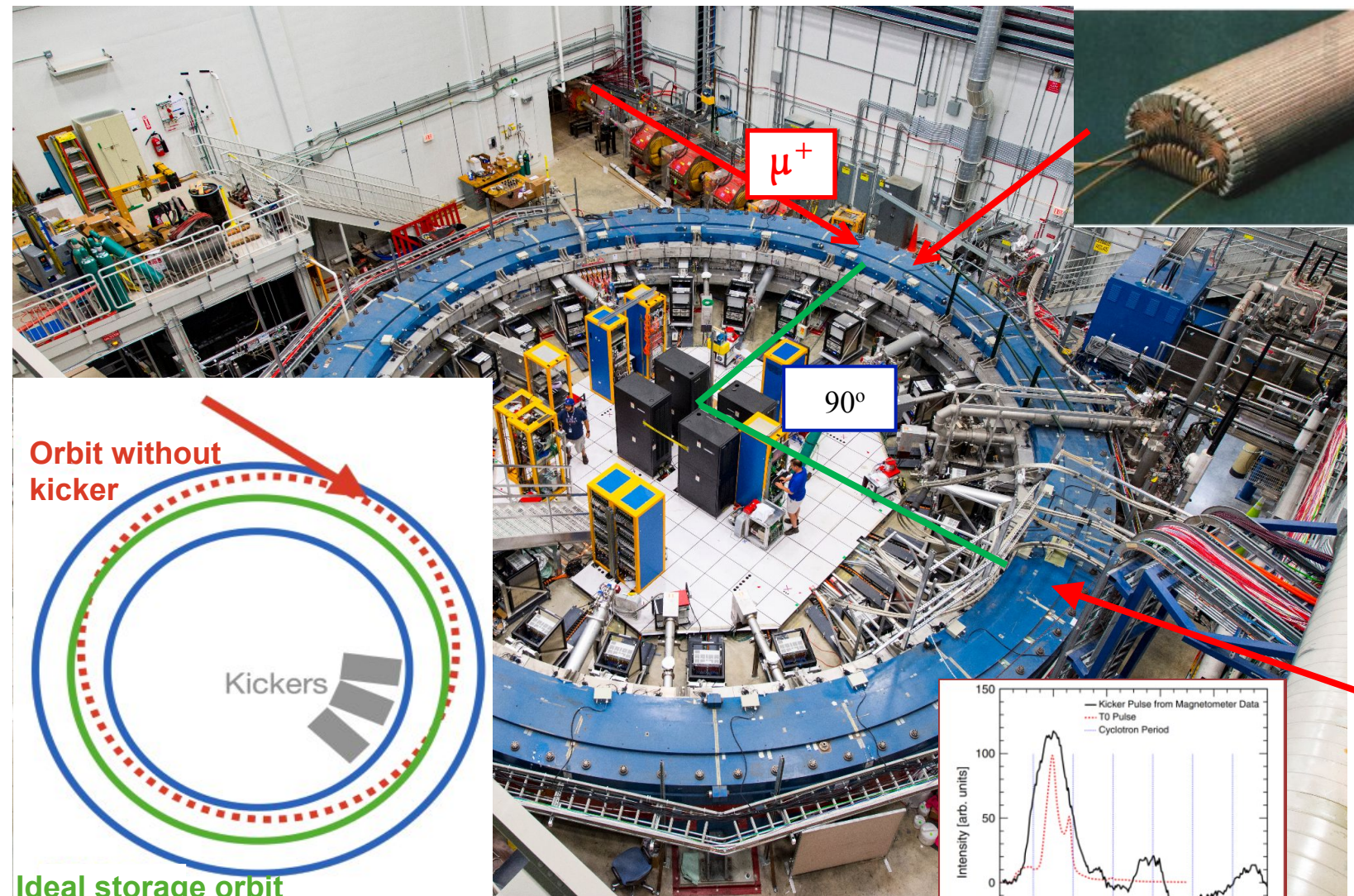
FNAL
2009 - 2023
0.14 ppm



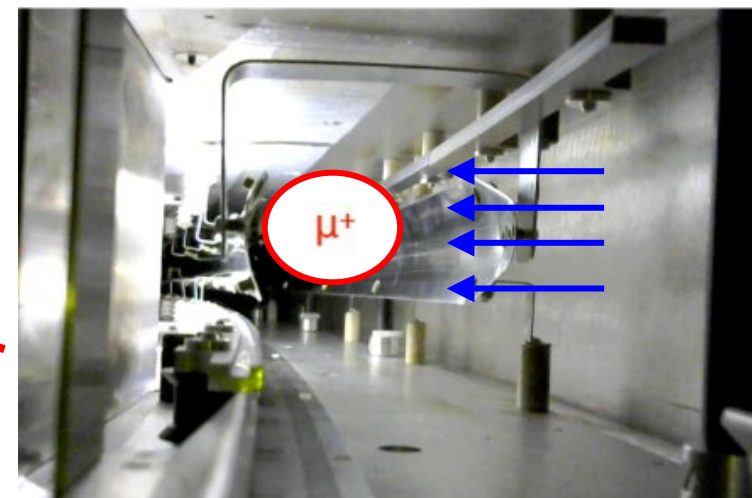
J-PARC
2009 - 2030s
0.45 ppm



Magnetic Kicker

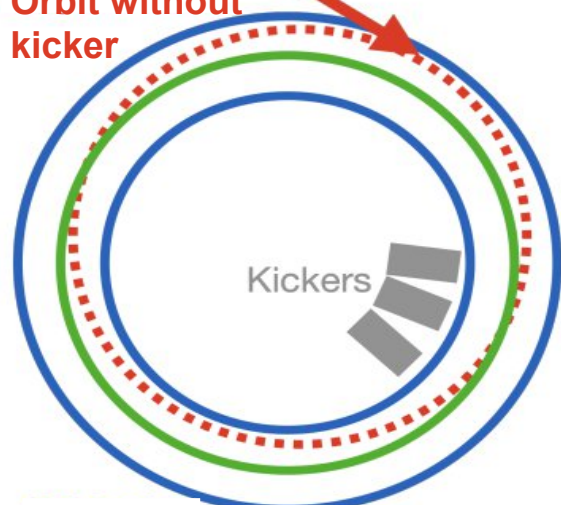


- For every 1.2 s, one fill consists:
 - 16 bunches of muon
 - boosted muon lifetime: 64 μs
 - Cyclotron period: 149.2 ns
 - Storage time: 700 μs
- Expected ~ 5000 stored muons in one fill.

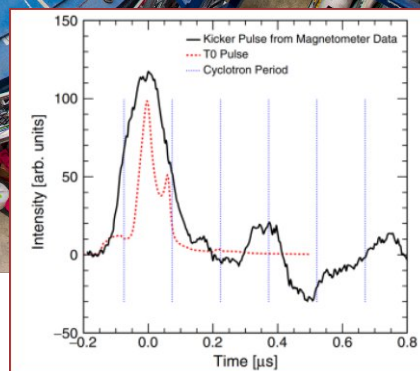


kicker magnets were used to correct the angular offset of muon momentum ($10.8_{<6>$ mrad)

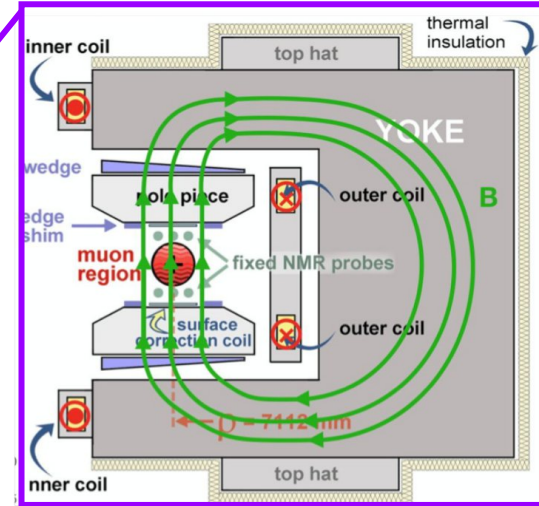
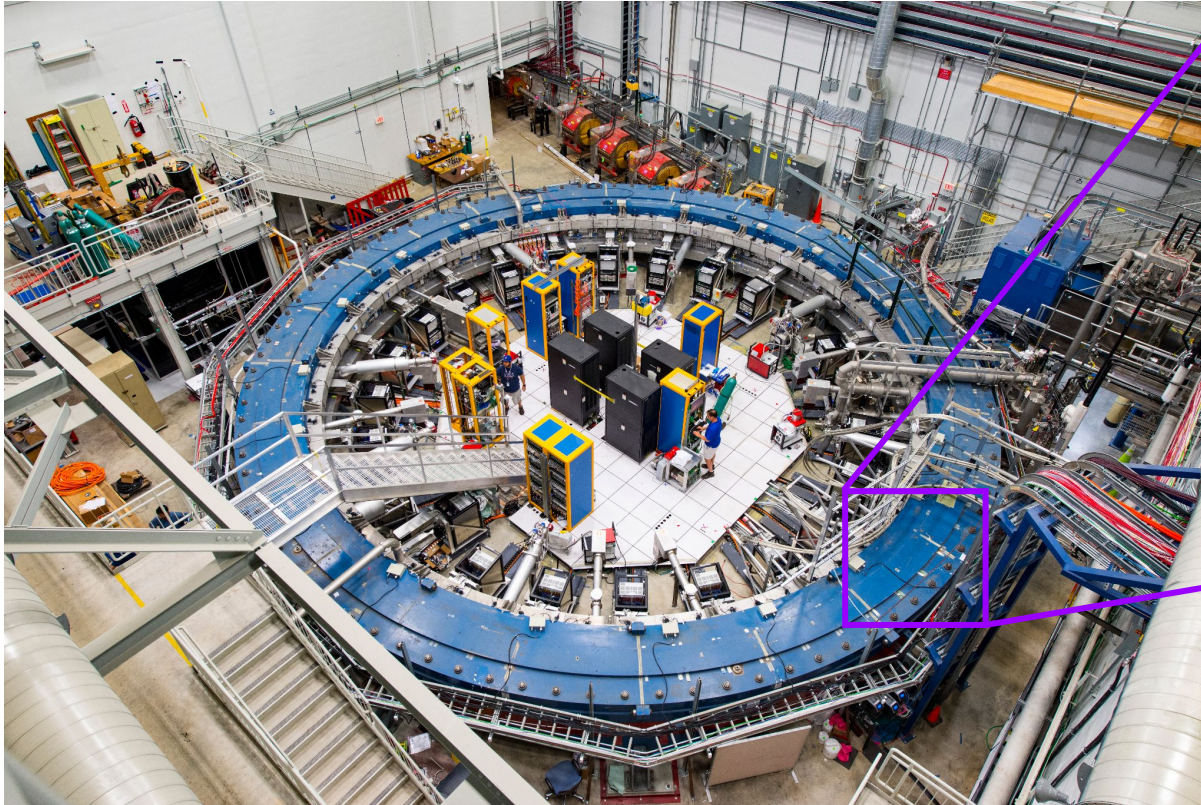
Orbit without kicker



Ideal storage orbit

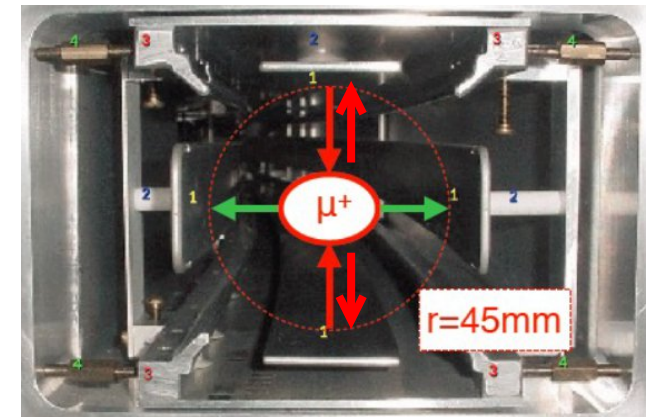


Dipole Magnetic Field

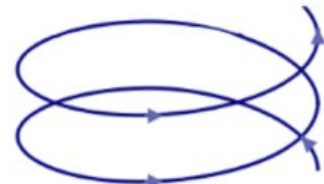


C-shape magnet faces toward interior of the ring, so that positrons from muon decay spiral inward unobstructed.

The ring dipole magnetic field of 1.45 Tesla, provide radial confinement.



However,

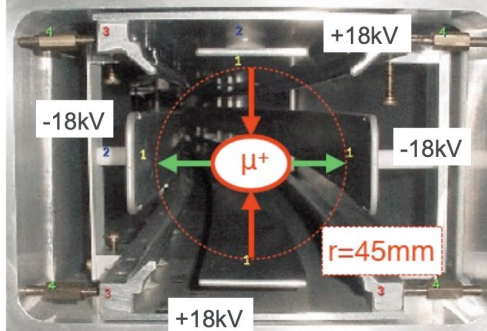
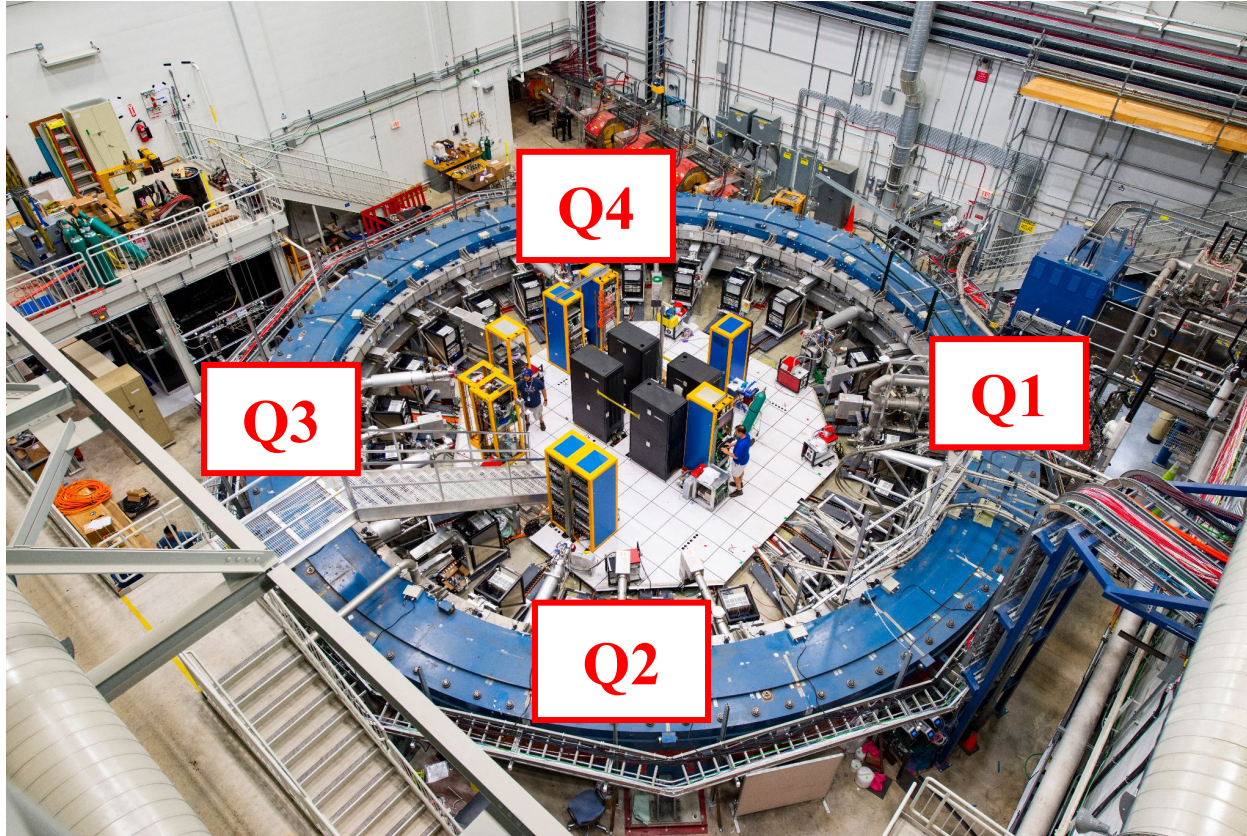


non-zero vertical momentum component without focusing

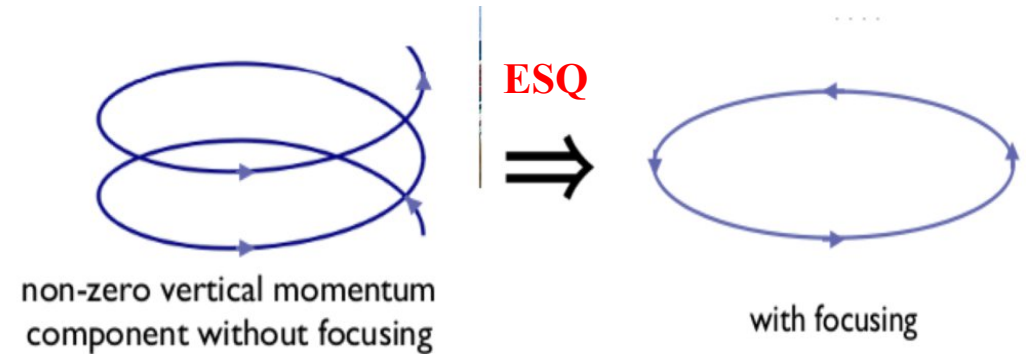
$$\vec{\omega}_a = -\frac{q}{m_\mu} \left[a_\mu \vec{B} - a_\mu \left(\frac{\gamma}{\gamma + 1} \right) (\vec{\beta} \cdot \vec{B}) \vec{\beta} \right]$$

non-negligible vertical oscillation

Electrostatic Quadrupoles



Uses Electrostatic Quadrupoles (ESQ) to provides weak focusing for vertical confinement.



The ESQ Covers 43% of the ring's circumference

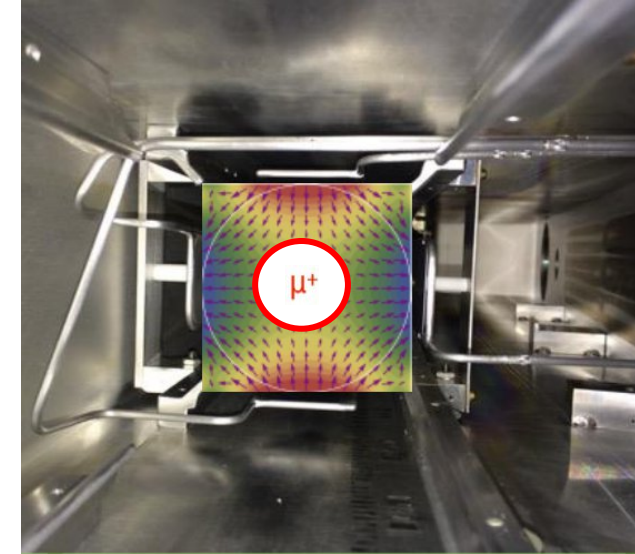
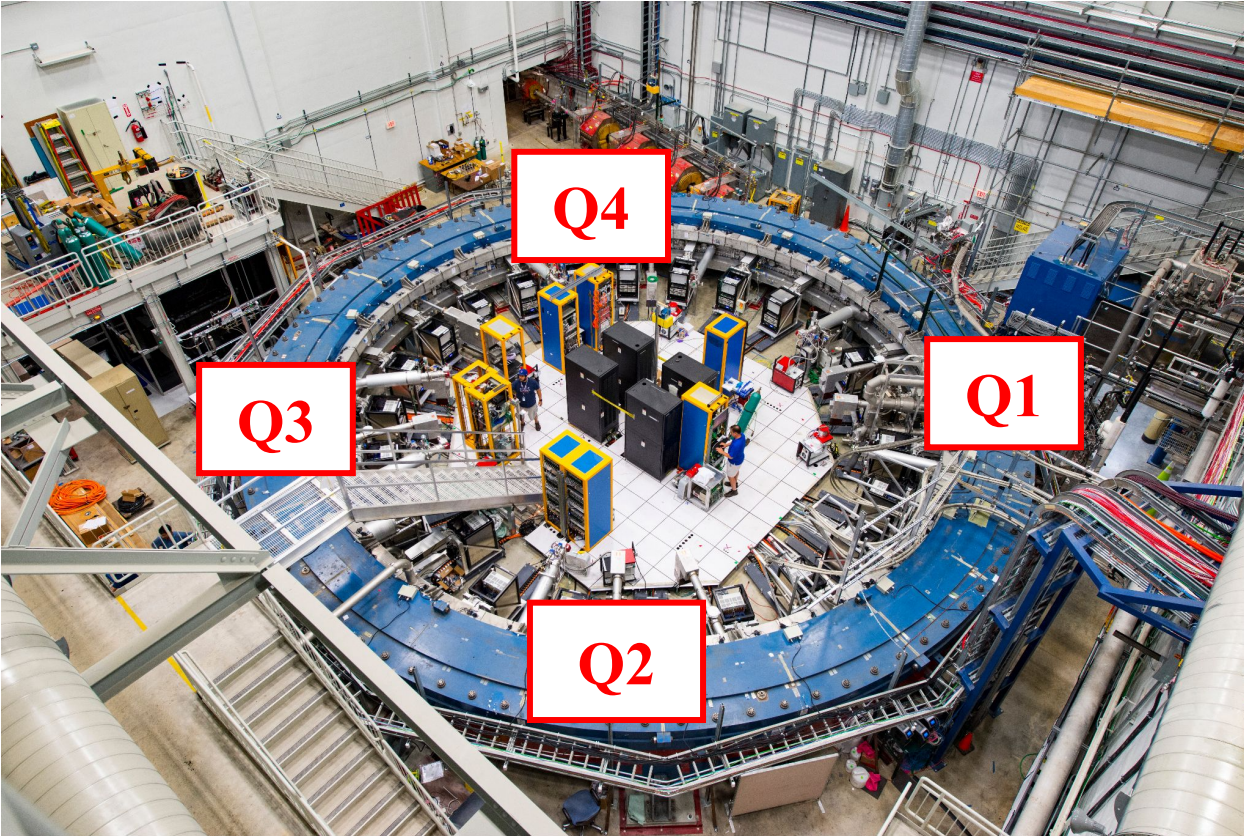
$$\vec{\omega}_a = -\frac{q}{m_\mu} \left[a_\mu \vec{B} - a_\mu \left(\frac{\gamma}{\gamma+1} \right) (\vec{\beta} \cdot \vec{B}) \vec{\beta} - \left(a_\mu - \frac{1}{\gamma^2 - 1} \right) \frac{\vec{\beta} \times \vec{E}}{c} \right]$$

ESQ ~ 0

However,

Muon experience motional magnetic field

Magic Momentum



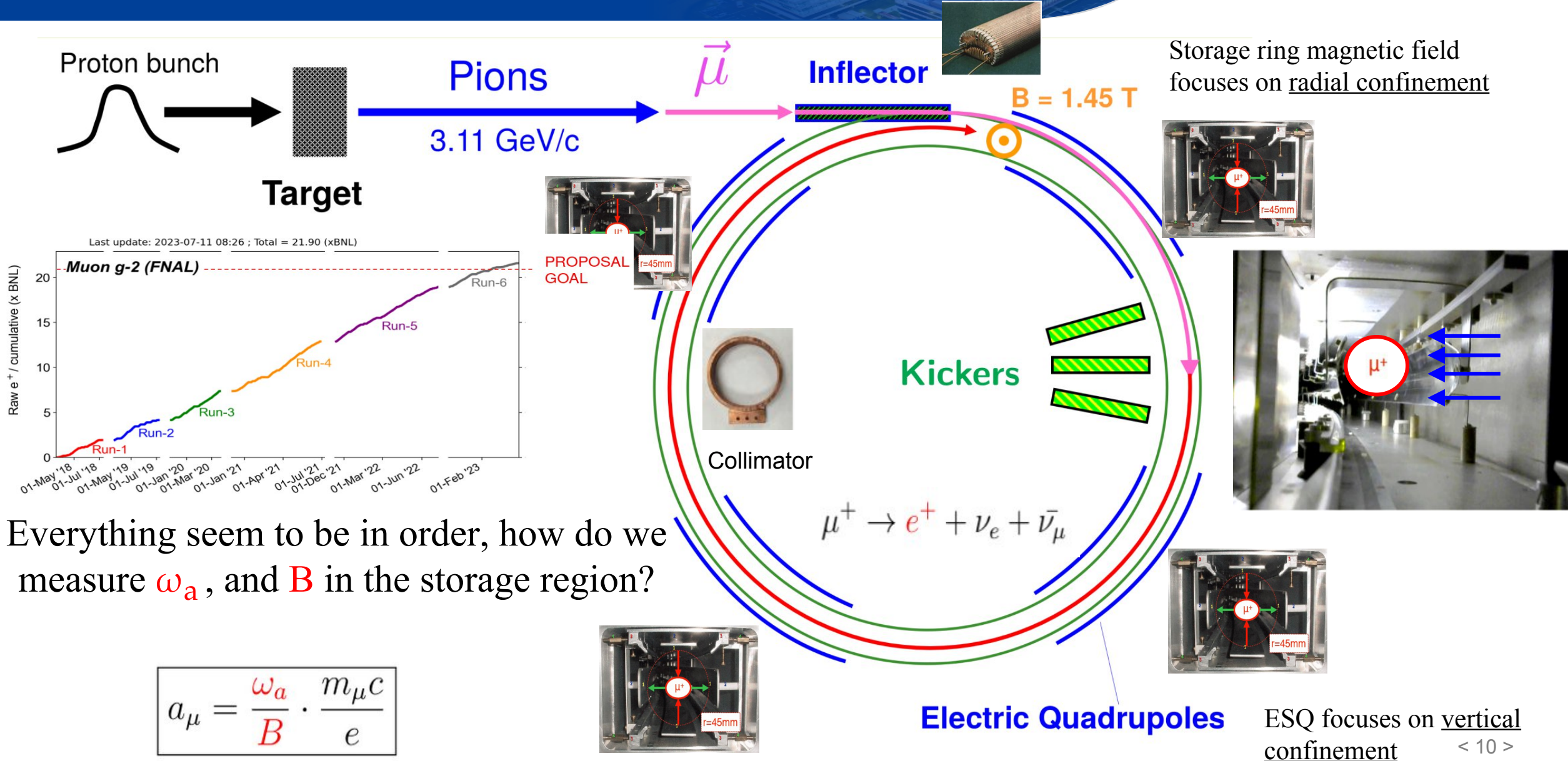
Cancel higher order contribution by allowing E-field vertical focusing at $p_\mu = 3.1$ GeV (**magic momentum**)

The non-zero pitch and motional field motivates the pitch and E-field Corrections.

$$\vec{\omega}_a = -\frac{q}{m_\mu} \left[a_\mu \vec{B} - a_\mu \left(\frac{\gamma}{\gamma+1} \right) (\vec{\beta} \cdot \vec{B}) \vec{\beta} - \left(a_\mu - \frac{1}{\gamma^2-1} \right) \frac{\vec{\beta} \times \vec{E}}{c} \right]$$

↗ **ESQ** ~ 0
↘ ~ 0 for $\gamma = 29.3$ ($p_\mu = 3.1$ GeV)

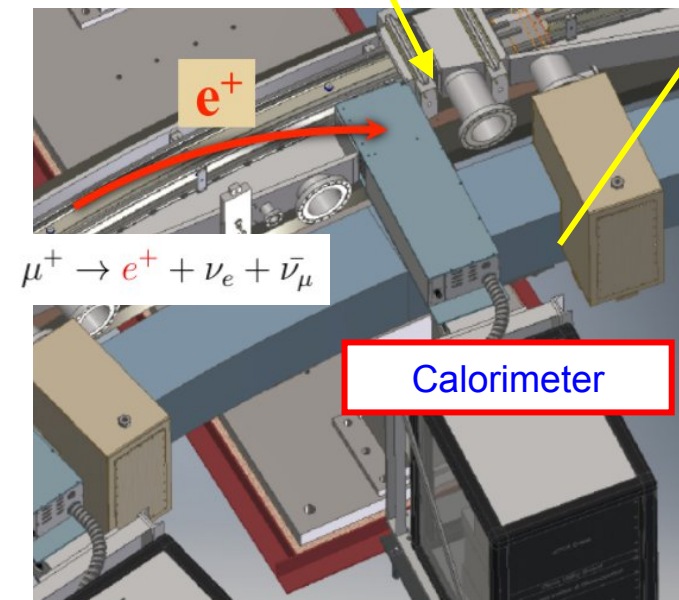
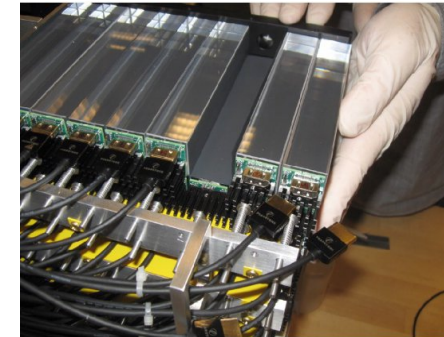
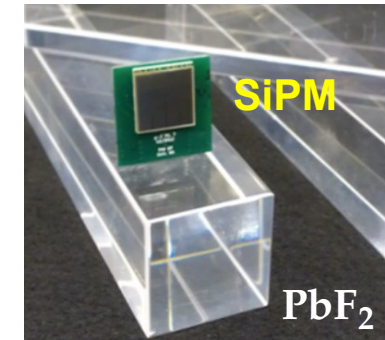
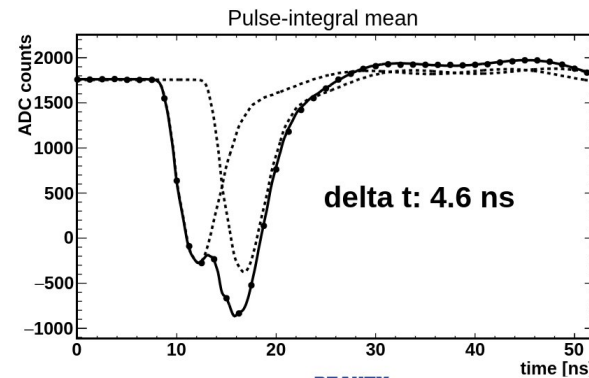
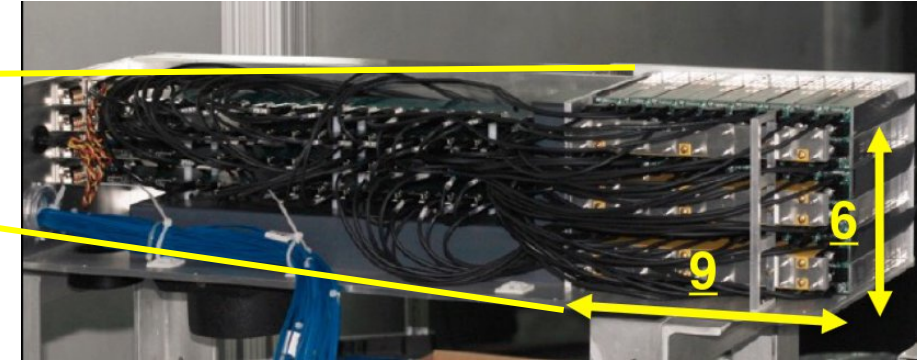
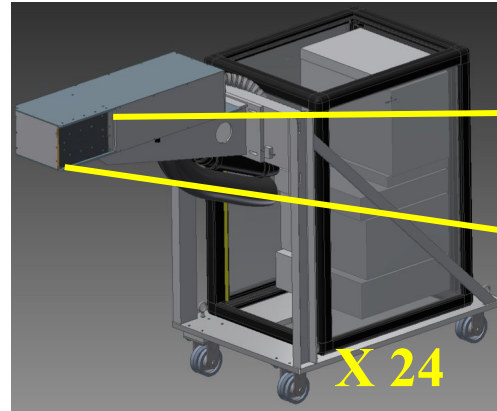
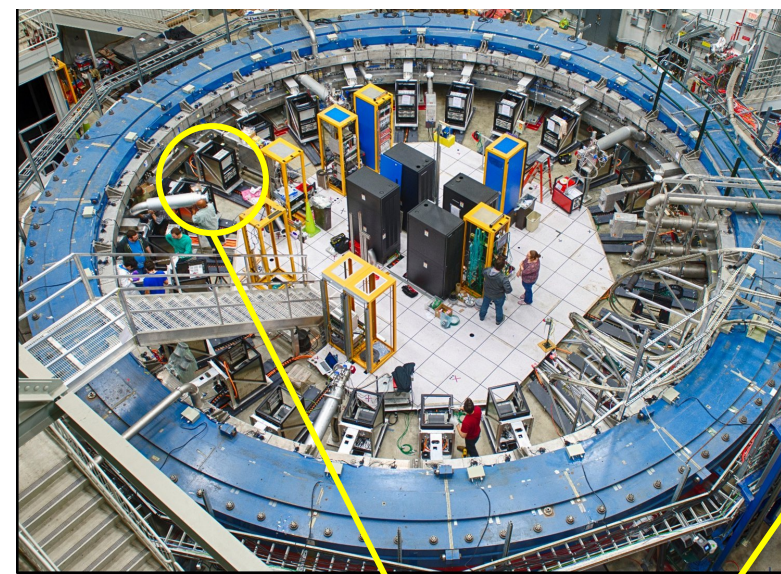
Stored Muon Beam



Everything seem to be in order, how do we measure ω_a , and B in the storage region?

$$a_\mu = \frac{\omega_a}{B} \cdot \frac{m_\mu c}{e}$$

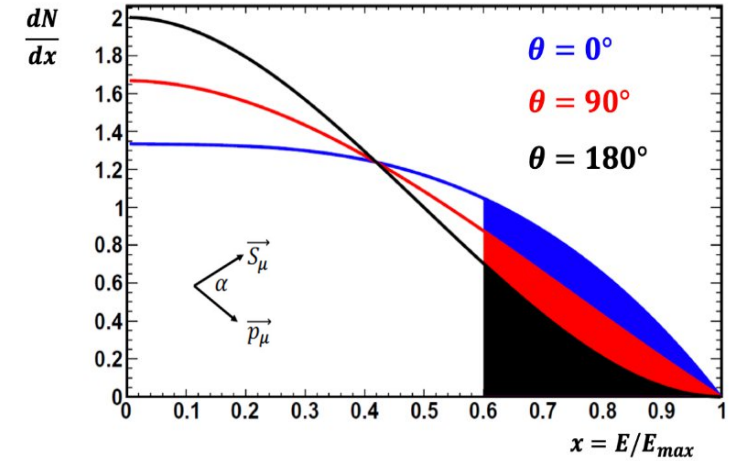
Positron Detection in Calorimeter



- Positrons from muon decays are detected in 24 calorimeters.
- Each PbF₂ crystal is read out by Geiger-mode avalanche photodiode (SiPM), > 99% operational in the experiment.
- Decay positron hit times and energies are derived from reconstruction of the waveforms.

ω_a Measurement

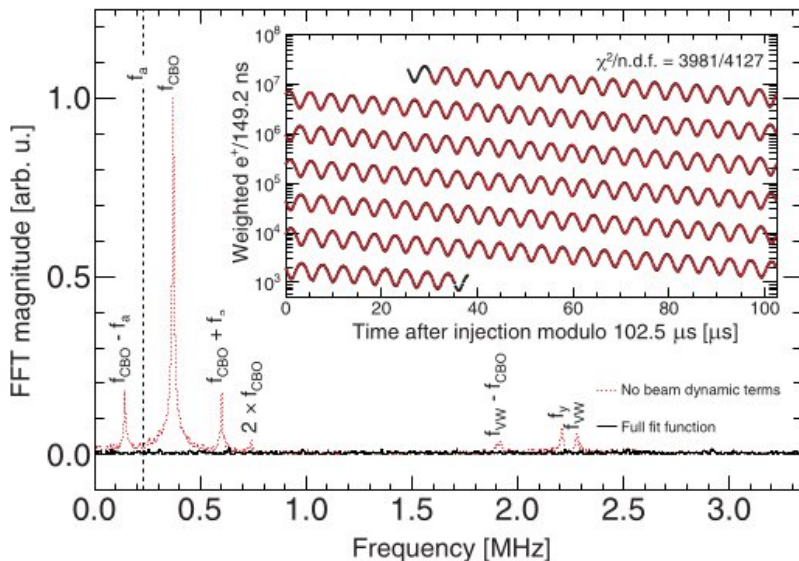
- Above certain energy threshold, the time distribution of detected positrons demonstrates the muons exponential decay, modulated by ω_a .
- Prior to a fit, the corrections are accounted for:
 - pile-up
 - Gain-like slow term due to reconstruction issues.
- The distribution is fitted to extract ω_a^m , including:
 - Coherent betatron oscillation (CBO) terms that distort the modulation signal.
 - Lost muons that distort the exponential shape of the distribution.



SJTU's contribution



YoungHao's poster
Zejia's poster



$$N(t) = N_0 \cdot e^{-t/\tau_\mu} [1 + A \cdot \cos(\omega_a^m \cdot t + \phi_0)]$$

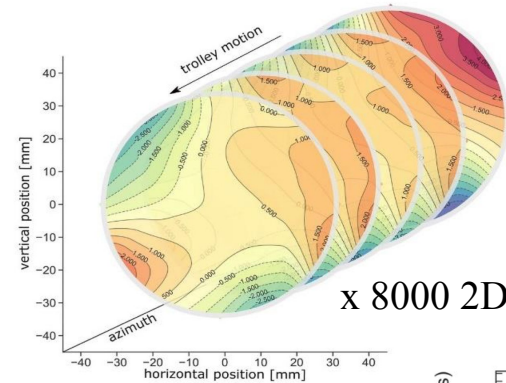
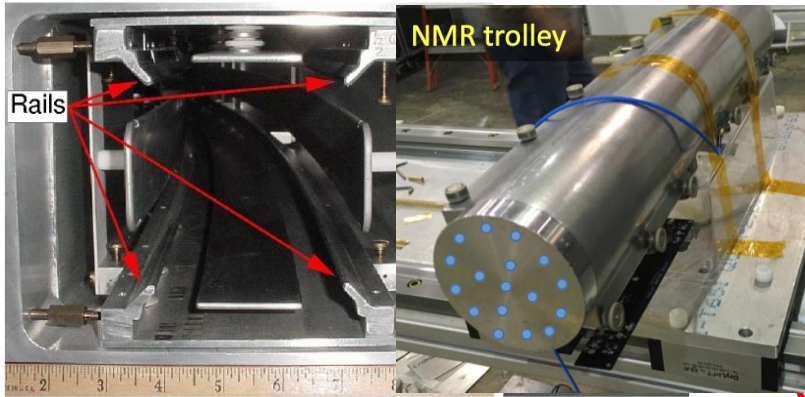


$$f(t) = N_0 \cdot N_x(t) \cdot N_y(t) \cdot N_{xy}(t) \cdot \Lambda(t) \cdot e^{-t/\gamma\tau_\mu} [1 + A_0 \cdot A_x(t) \cdot \cos(\omega_a^m \cdot t + \phi_0 \cdot \phi_x(t))]$$

Magnetic Field Measurement

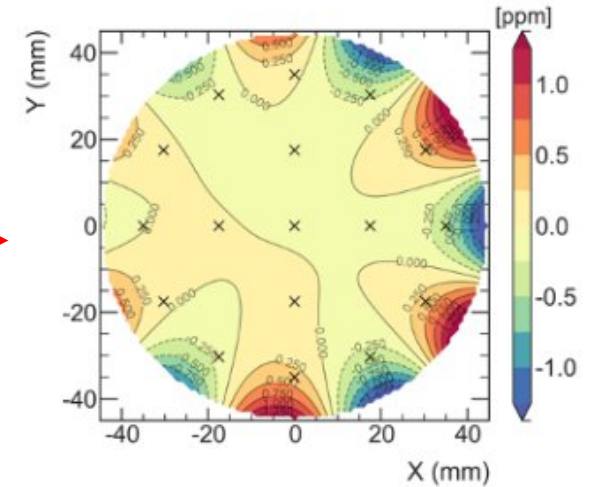
- A field map in the storage region is interpolated using fixed probes and trolley data.

Variation < 1 ppm



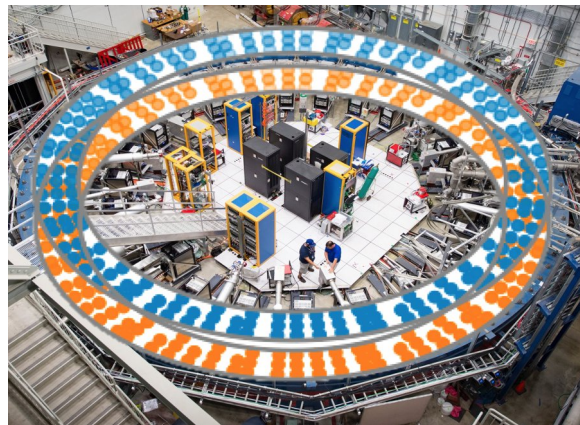
x 8000 2D field maps

Azimuthally Averaged

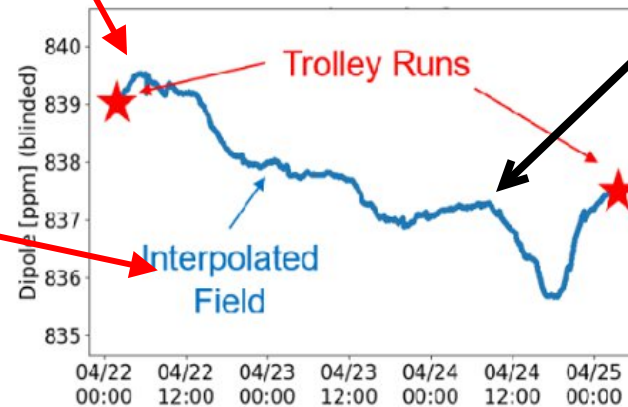
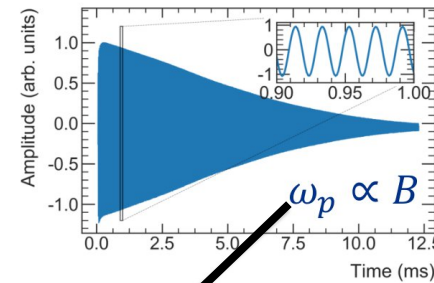


$$\omega_p(x, y, \phi)$$

Trolley “Run”, with 17 pNMR probes, every 3 days (No Beam present)

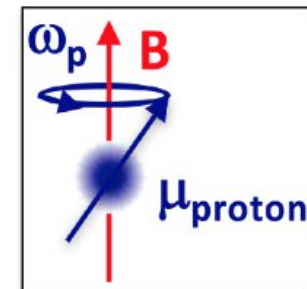


378 fixed probes monitor field (Beam or no beam time)

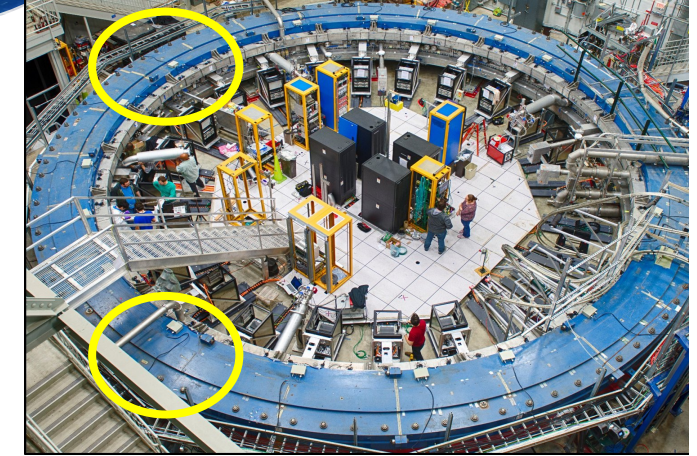
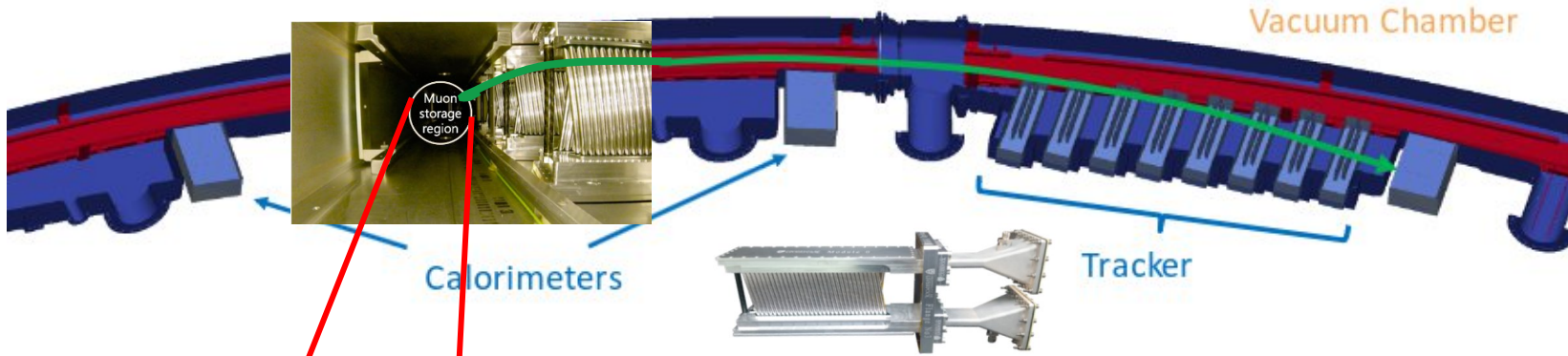


Magnetic field is expressed in term of the shielded proton precession frequency, ω_p'

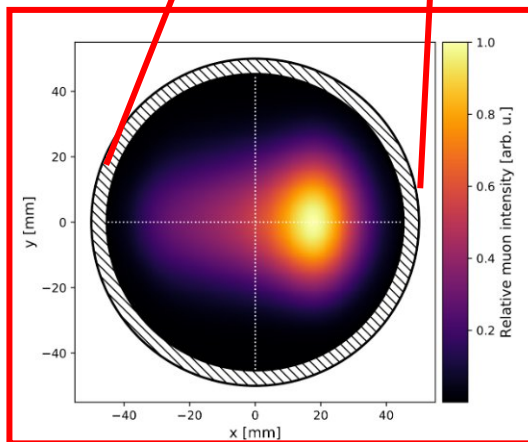
$$B = \frac{\hbar\omega_p}{2\mu_p}$$



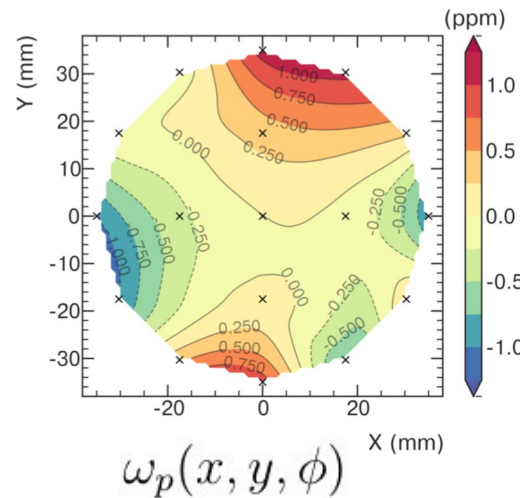
Muon Decay Position Reconstruction



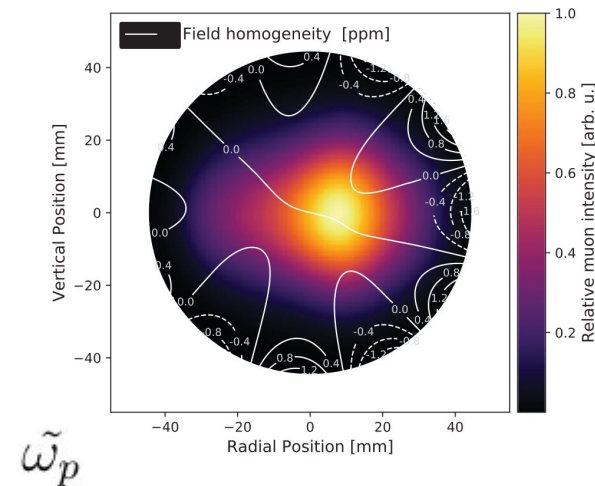
- The 2 tracker stations track the positron decay, extrapolates to the muon decay position, thus measuring the muon distribution $M(x,y,\phi)$.
- The field map is then weighted with the muon distribution measured in the storage region:



X



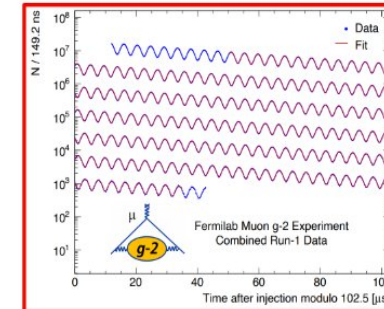
=



Visualizing the Measurement

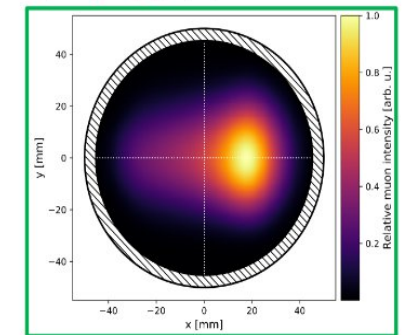
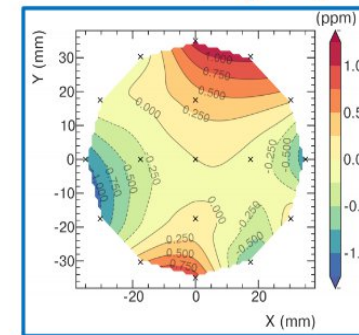
- The ω_a^m is extracted from the fit to the time distribution of decayed positron.
- The $\tilde{\omega}'_p$ is obtained from weighting ω'_p with M.

$$a_\mu = \frac{\omega_a}{B} \cdot \frac{m_\mu c}{e} \quad \longrightarrow \quad a_\mu^{\text{Exp}} = \left[\frac{\omega_a}{\tilde{\omega}'_p} \right] \left[\frac{\mu_p m_\mu g_e}{\mu_e m_e 2} \right] \quad \mathcal{R}'_\mu = \frac{\omega_a}{\tilde{\omega}'_p(T_r)} = \frac{f_{\text{clock}} \omega_a^m (1 + C_e + C_p + C_{ml} + C_{pa})}{f_{\text{calib}} \langle \omega_p(x, y, \phi) \times M(x, y, \phi) \rangle (1 + B_k + B_q)}$$



External factors are of high precision, (25ppb)

Quantity	Source	Uncertainty (ppb)
$g_e/2$	Quantum electron cyclotron	0
μ_p/μ_e	Hydrogen spectroscopy	11
m_μ/m_e	Muonium hyperfine splitting	22

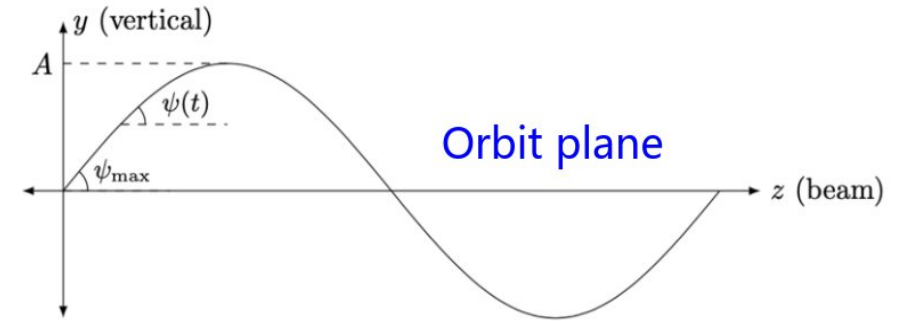


- The f_{clock} and f_{calib} are blinding factors.
- The ω_a^m ($\tilde{\omega}'_p$) receives several corrections from the **beam dynamics** (transient fields).
- Transient field's correction:
 - B_k : Correction due to kicker eddy current.
 - B_q : Correction due to vibration caused by quad pulsing.

Corrections related to Frequency Shift

These corrections account for the shift effect in ω_a^m

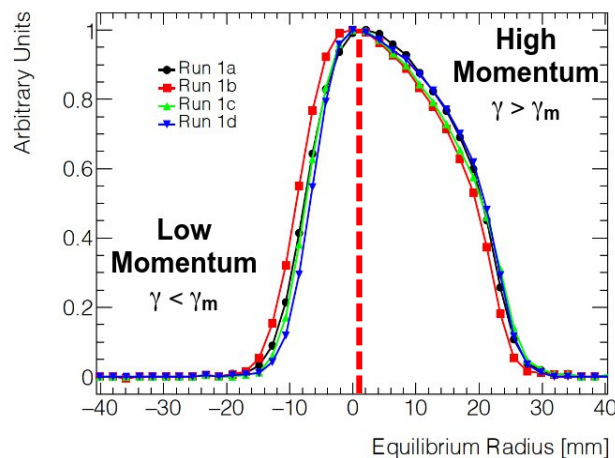
$$\frac{\omega_a}{\omega_p} = \frac{\omega_a^m}{\omega_p^m} \frac{1 + C_e + C_p + C_{pa} + C_{dd} + C_{ml}}{1 + B_k + B_q}$$



Muon trajectory

Electric field Correction C_e :

- Not all muons are at magic momentum, due to finite width of momentum distribution.
- Radial distribution is measured using timing data from calorimeters.



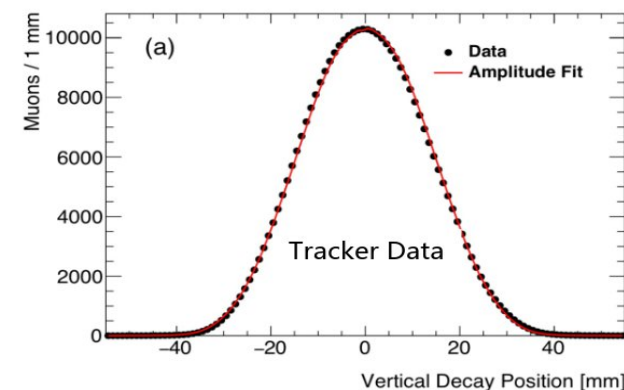
$$C_e \approx 2n(1-n)\beta_0^2 \frac{\langle x_e^2 \rangle}{R_0^2}$$

$$C_e \approx O(500 \text{ ppb})$$

$$\delta C_e \approx O(30 \text{ ppb})$$

Pitch correction C_p

- non-zero pitch motivates this correction.
- The vertical betatron oscillation is measured from the tracking detectors.



$$C_p \approx \frac{n \langle y^2 \rangle}{2 R_0^2} = \frac{n \langle A^2 \rangle}{4 R_0^2}$$

$$C_p \approx O(200 \text{ ppb})$$

$$\delta C_p \approx O(5 \text{ ppb})$$

Corrections related to Phase Shift

These corrections account for the shift in ϕ_0 over time.

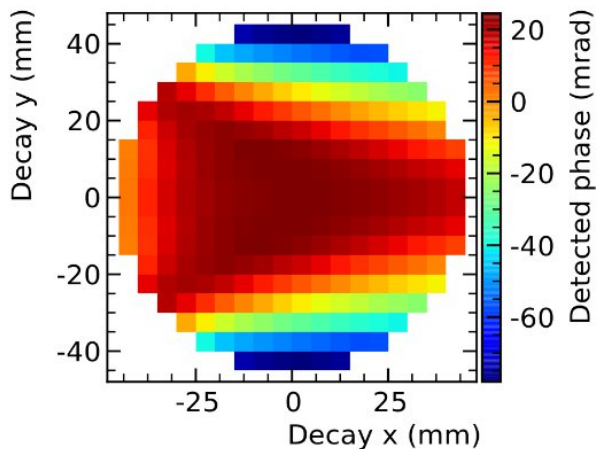
$$\frac{\omega_a}{\omega_p} = \frac{\omega_a^m}{\omega_p^m} \frac{1 + C_e + C_p + C_{pa} + C_{dd} + C_{ml}}{1 + B_k + B_q}$$

Lost muon Correction, C_{ml}

- low momentum muon tend to be lost, the average stored muon phase will change over time. $\frac{d\langle\phi\rangle}{dt} = \frac{d\langle\phi\rangle}{d\langle p\rangle} \left(\frac{d\langle p\rangle}{dt} \right)_{lm}$ $C_{ml} = 0(3)$ ppb

Phase-acceptance correction, C_{pa} :

- Correlation between muon decay position and ϕ_0 .
- Measuring the beam's spread over time and simulating how it affects the average phase at the calorimeters.



$$C_{pa} = -27(13) \text{ ppb}$$



Jun kai's poster

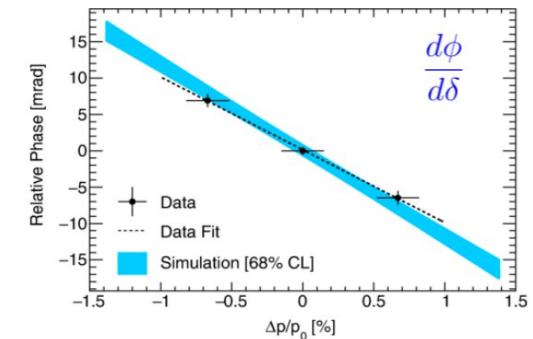
SJTU's contribution

Differential decay Correction, C_{dd} :

- low momentum has shorter lifetime, the change in momentum over time couples to phase-momentum correlation (from lost muon) causes bias in ϕ_0 .

$$\frac{d\langle\phi\rangle}{dt} = \frac{d\langle\phi\rangle}{d\langle p\rangle} \left(\frac{d\langle p\rangle}{dt} \right)_{dd} \approx \frac{d\phi}{d\delta} \frac{1}{\gamma_0 \tau_\mu} \sigma_\delta^2$$

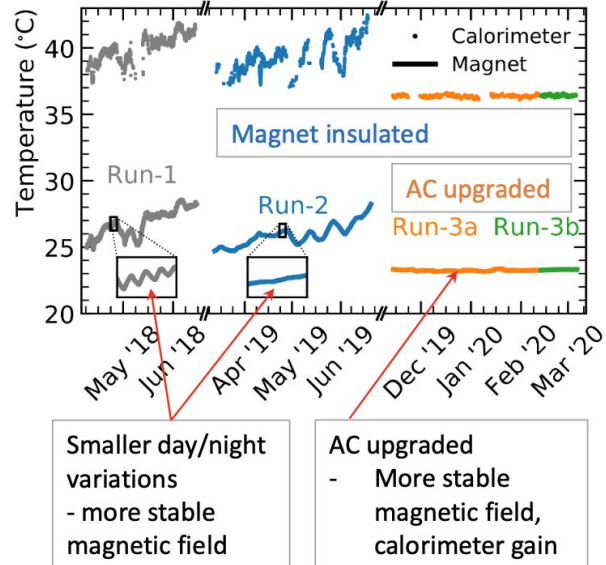
$$C_{dd} = -15(17) \text{ ppb}$$



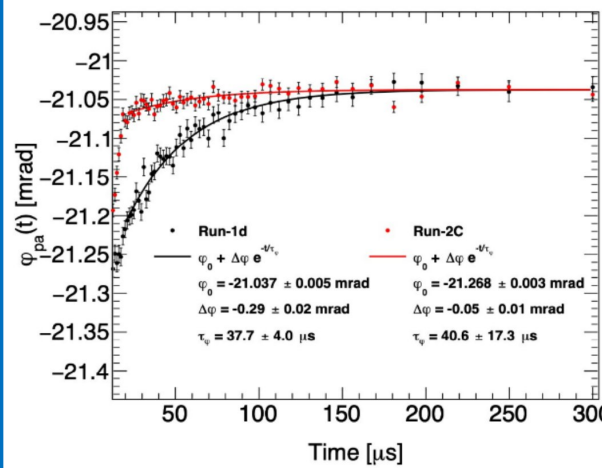
SJTU's contribution

Improvements for Run-2/3

Hall/Ring temperature stabilized

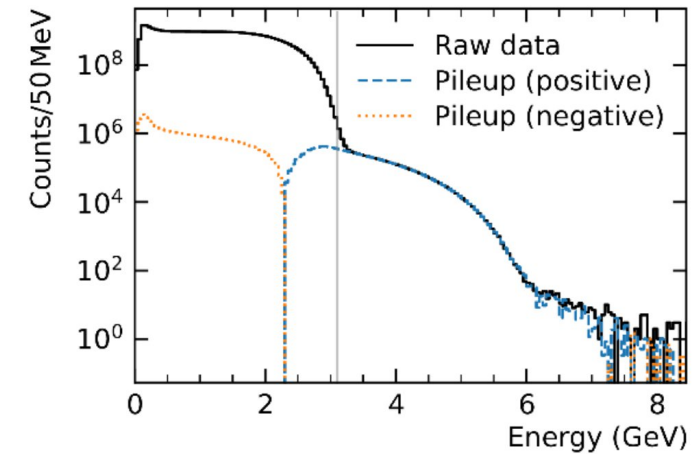


Fix failed HV resistor in quad

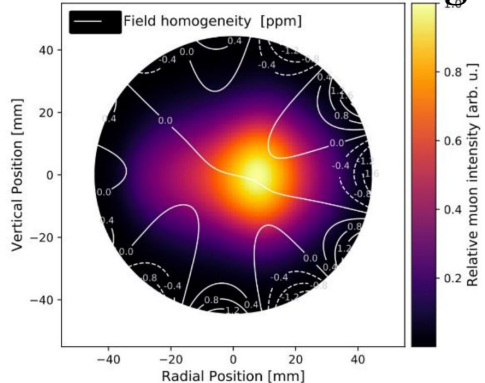


- Stable beam
- small C_{pa}
- lower muon loss, less C_{ml}

Improved pileup reconstruction

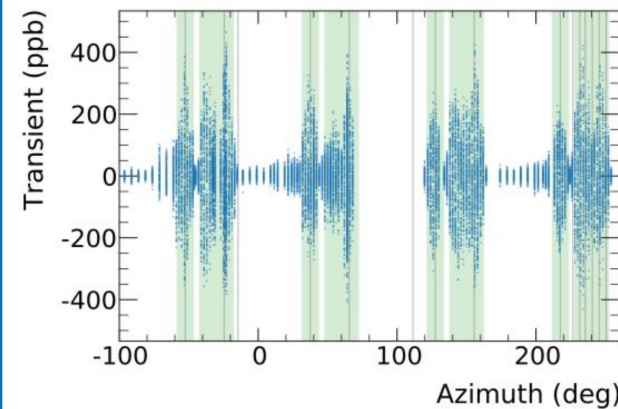


Stronger kick



- More center beam.
- Better C_e measurement
- higher Homogeneity of muon to magnetic field.

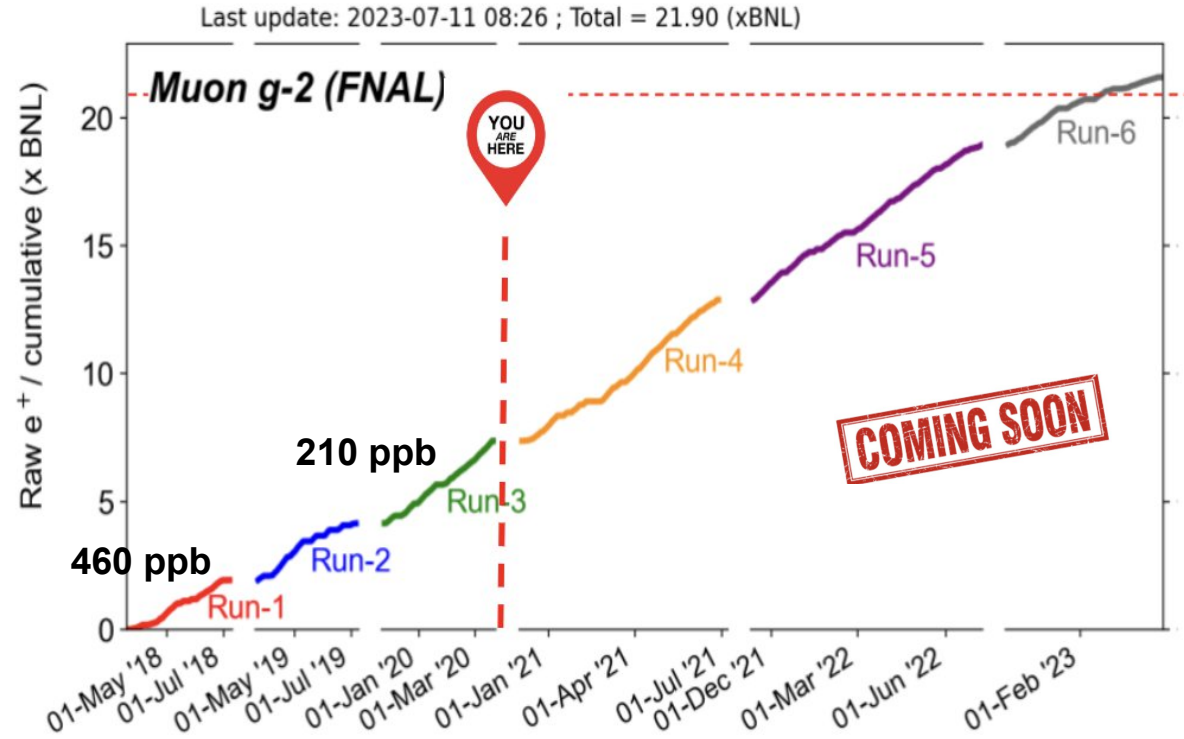
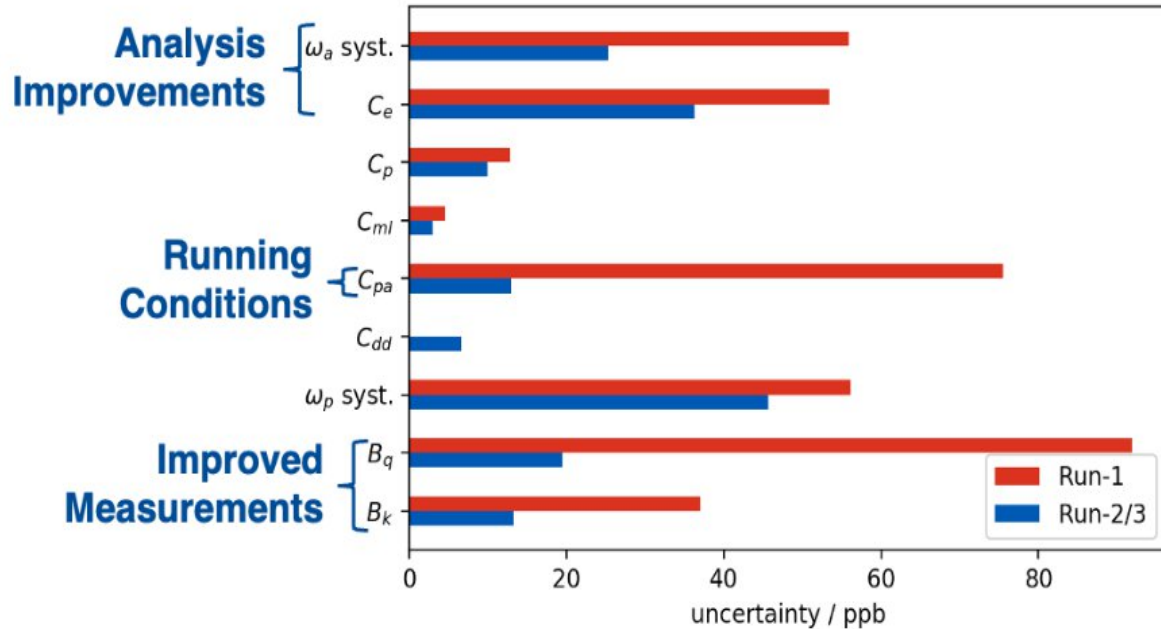
Improved transient field measurement



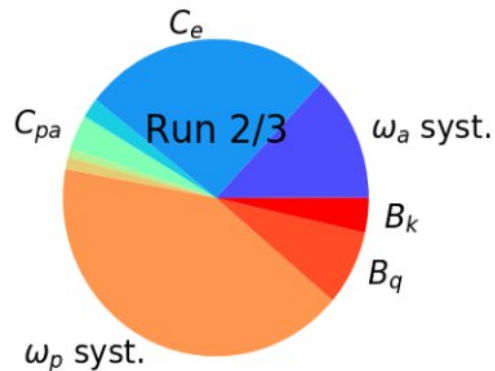
- Complete quad transient field measurement.
- Improved kicker transient field measurement with fiber magnetometer.

Achieved Precision and g-2 Data

$$\frac{\omega_a}{\omega_p} = \frac{\omega_a^m}{\omega_p^m} \frac{1 + C_e + C_p + C_{pa} + C_{dd} + C_{ml}}{1 + B_k + B_q}$$



After improvements, total systematic comes from **multiple sources**



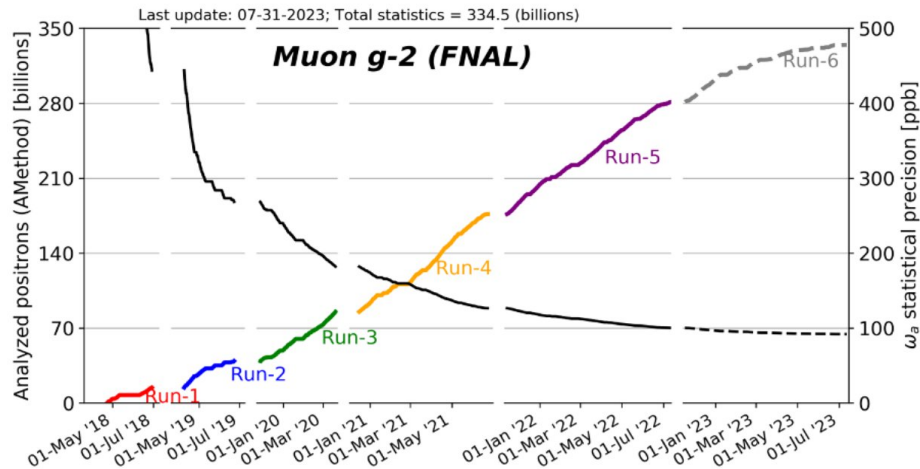
[ppb]	Run-1	Run-2/3
Stat.	434	201
Syst.	157	70



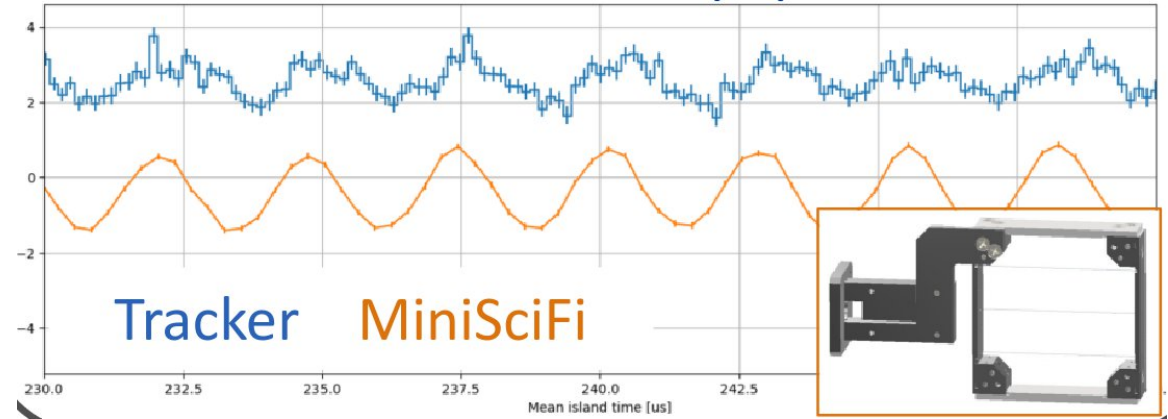
Surpassing proposed goal of the experiment!

X 2.2 improvement

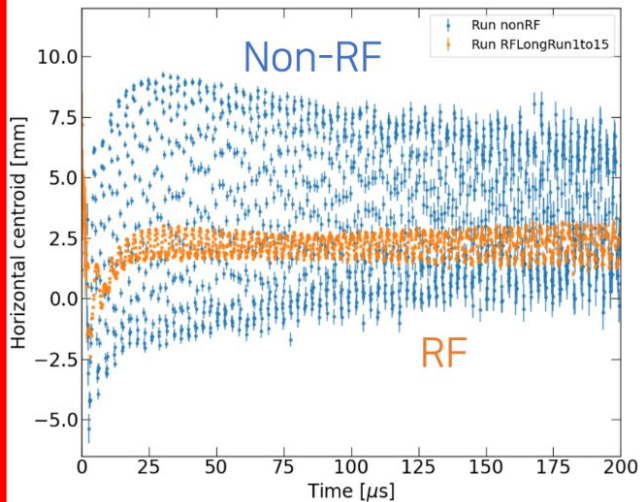
Improvements for Run-4+



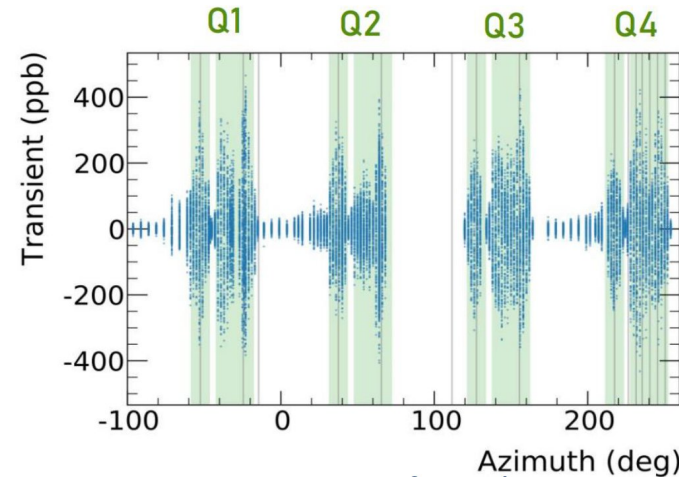
Higher Statistical power $\sim x 4$ Run-1/2/3



Additional new detectors employed in Run-4/5/6



Continuous improved experimental condition.
Quad RF in Run-5 reduces CBO amplitude

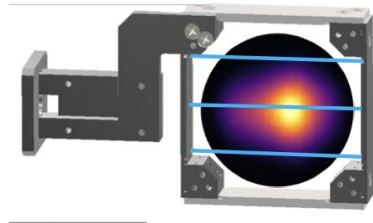
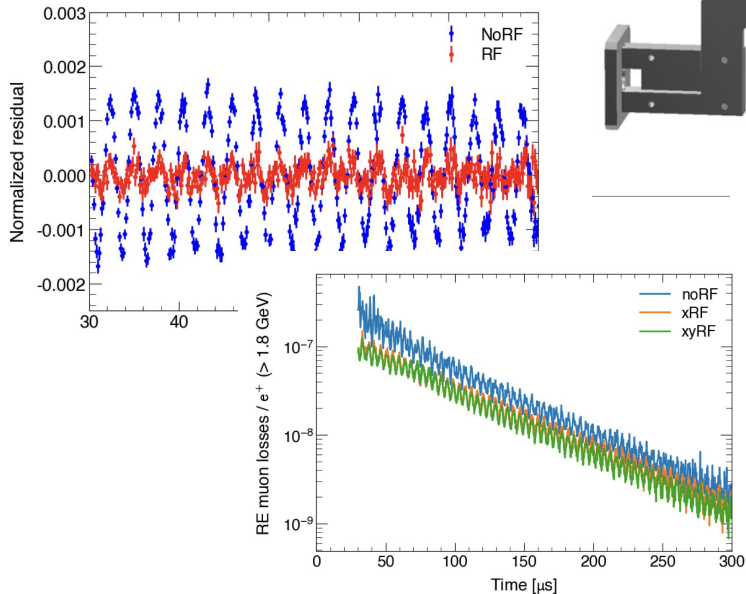
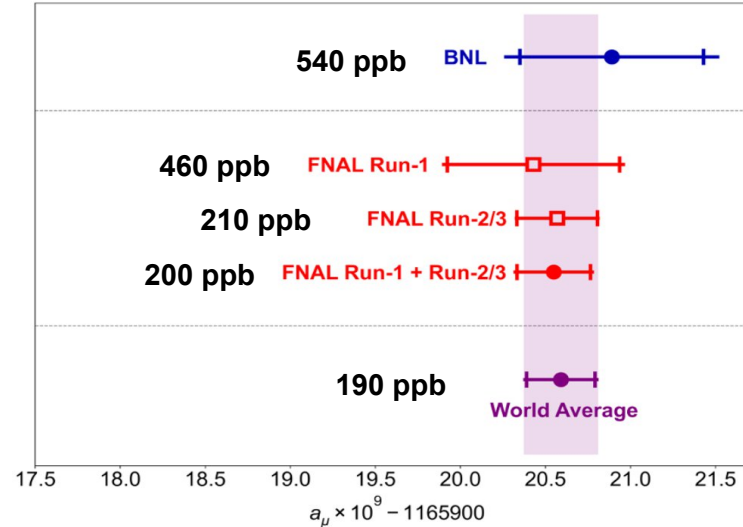


Run-1 Measurement
Run-2+ Measurements

Throughout measurement of quad main and transient fields continue post-Run6

Conclusion and Outlook

- Run-2/3 analysis improves uncertainties by a factor of 2.2, in particular, the total systematic uncertainty surpasses proposed goal (100 ppb)!
- Analysis efforts on Run 4/5/6 data are on the way, full result expected to be released in 2025. (on track to achieve/surpass 140 ppb!)
- Theoretical efforts:
 - Lattice QCD results are under strict scrutiny.
 - Clarification among collaboration on the 5σ difference with CMD-3 is ongoing.



STAY TUNED!

Improvements for Run-2/3

- Hall/Ring temperature stabilized
- Fix failed HV resistor in quad
- Improved pileup reconstruction

Improvements for Run-4+

- Stronger kick
- Higher Statistical power ~ 4 Run-1/2/3
- Additional new detectors employed in Run-4/5/6

Tracker MiniSciFi

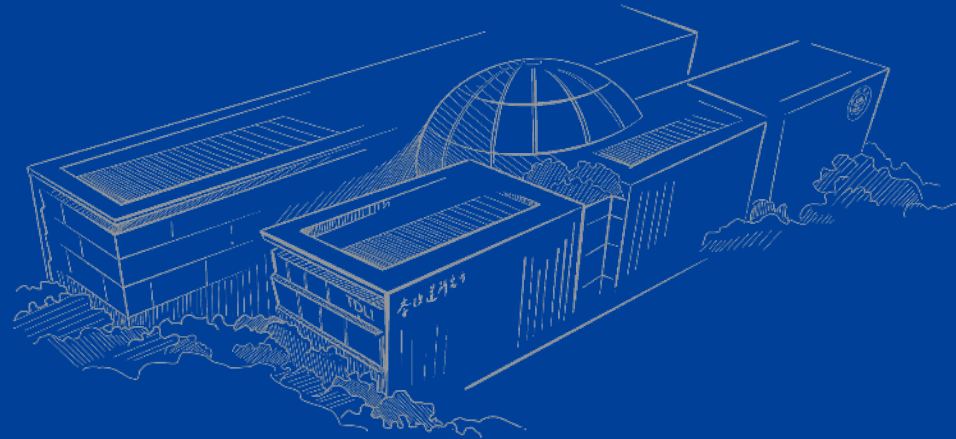
Run-1 Measurement Run-2+ Measurements

Throughout measurement of quad main and transient fields continue post-Run6

Continuous improved experimental condition. Quad RF in Run-5 reduces CBO amplitude

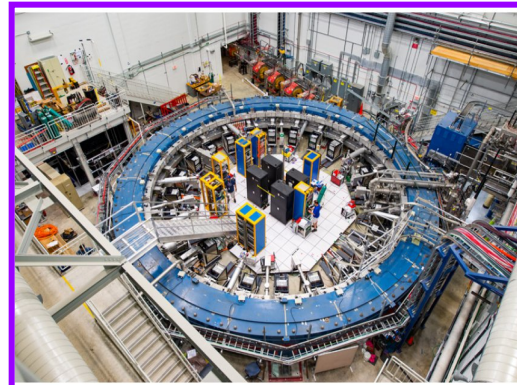
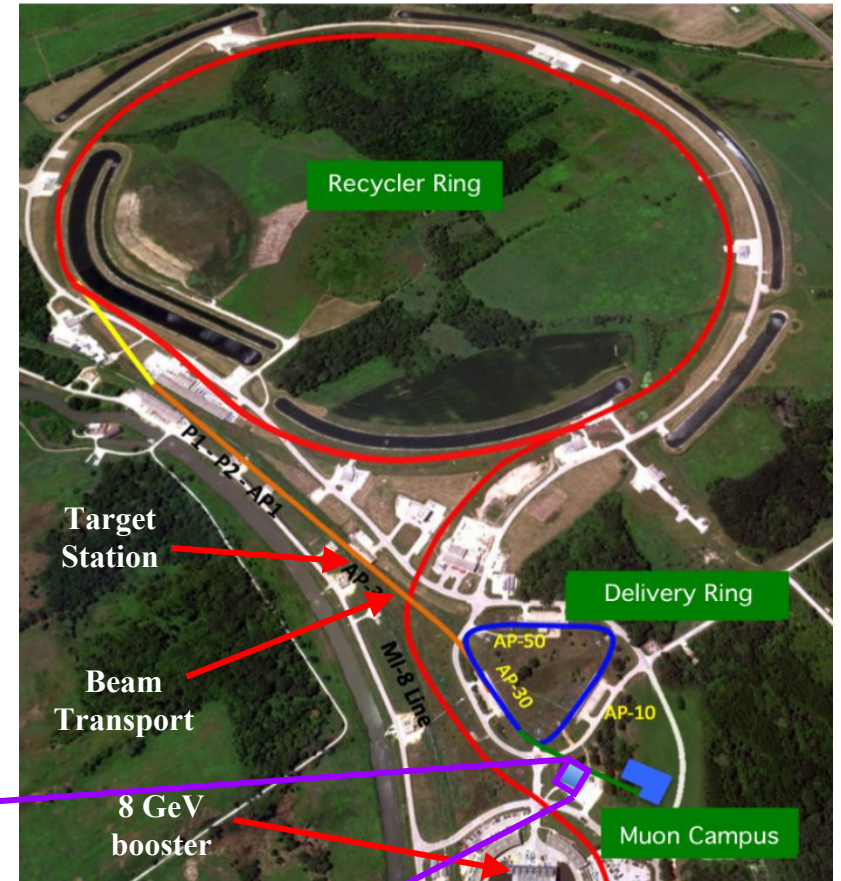


Backup



The FNAL Accelerator Complex

- LINAC produces 400 MeV proton beams
- Protons are accelerated to 8 GeV in Booster.
- Protons are batched into Recycler Ring, transported one at a time to the Target Station.
- Protons are smashed onto the nickel target, producing π^+ particles.
- Protons, μ^+ , π^+ beam enters delivery ring.
- Proton aborted, π^+ decays away.
- μ^+ beam is selected in momentum, 3.094 GeV/c.
- polarized μ^+ ($\sim 96\%$) are extracted and entered g-2 storage ring.

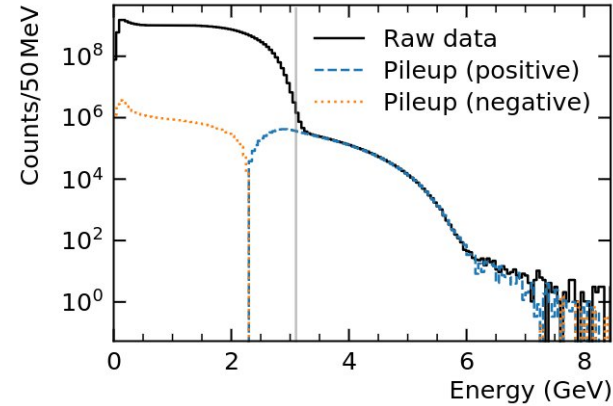
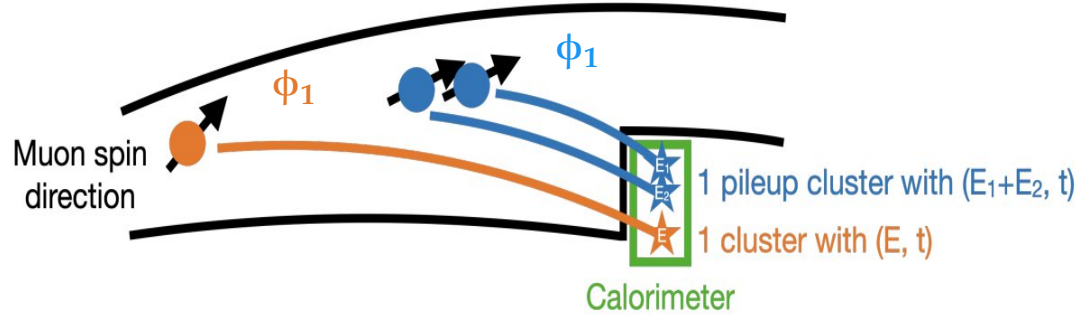


Skip this

- g-2 storage ring:
 - 7.1 meter radius storage ring.
 - 1.45 Tesla uniform magnetic field.

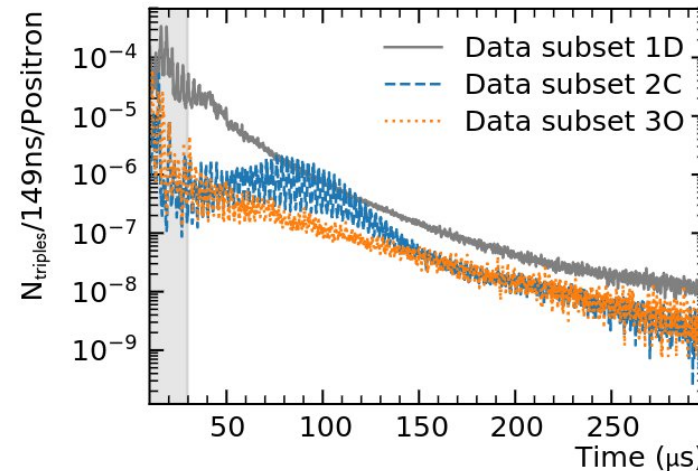
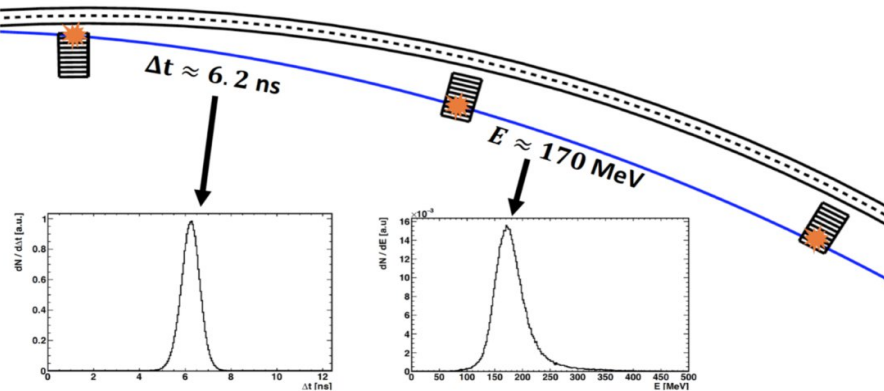
Pile-up and Lost Muon

- Low energy positrons with different phase measured in calorimeter, contributing to **pile-up event**; compares to **high energy positron**, a **single event**.



pileup model
uncertainty, ~ 3 ppb

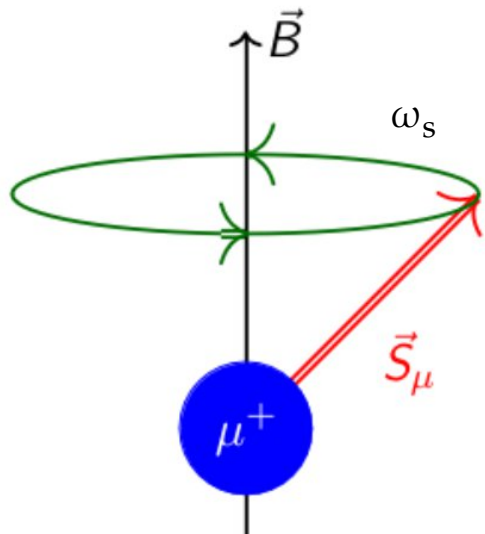
- Muons impact on vicinity of the SR, losses energy, exits the SR before decaying into positrons.
- Lost muons introduce time-dependent distortion of measured positrons.



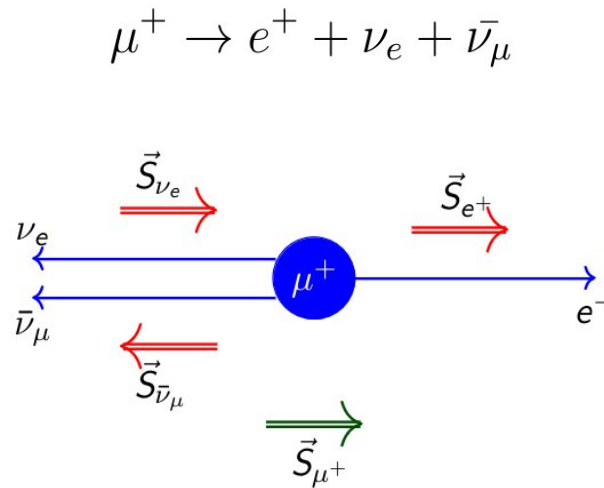
Muon lost time
distribution for different
sub-datasets.

Parity Violation in Muon Decay

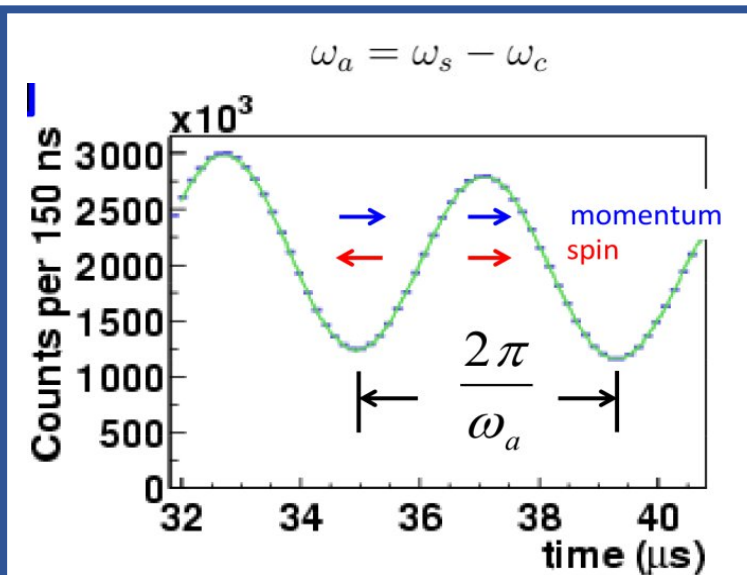
- Parity Violation provides access to study the ω_a in the storage ring.
- Highest energy positron has the strongest correlation with its momentum and muon spin direction (Vice Versa)



Muon spin precesses in magnetic field



Emitted positron's direction follows muon spin's



Number of high energy positron detected

External Factors

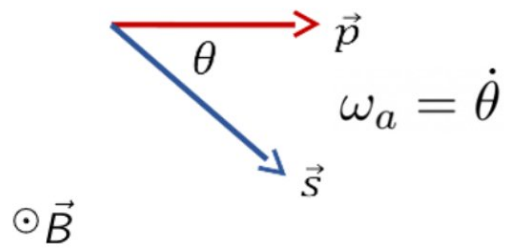
$$a_{\mu}^{\text{Exp}} = \left[\frac{\omega_a}{\tilde{\omega}_p} \right] \frac{\mu_p}{\mu_e} \frac{m_{\mu}}{m_e} \frac{g_e}{2}$$

- ω_p Larmor precession frequency of the free proton
- μ_p is the proton's magnetic dipole moment
- μ_e is the electron's magnetic dipole moment
- g_e is the g-factor for electron.

Muon Magnetic Anomaly in SR

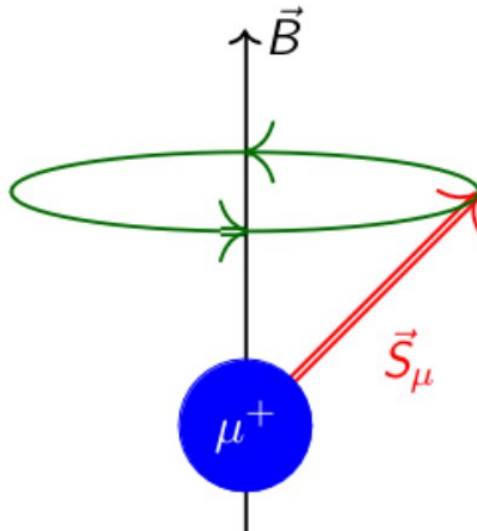
Measuring the difference between spin precession and cyclotron frequencies:

Anomalous spin frequency for spin vector precession



$$\vec{\omega}_a = a_\mu \frac{e}{m_\mu c} \vec{B}$$

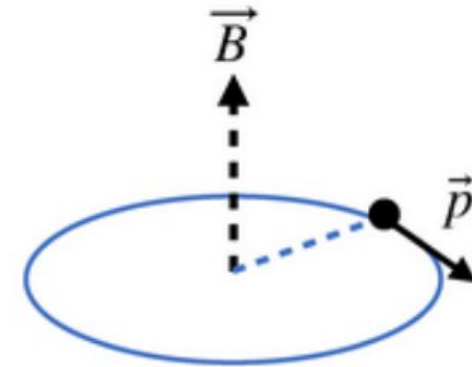
Larmor frequency for spin vector precession



$$\vec{\omega}_s = g_\mu \frac{e}{2m_\mu} \vec{B}$$

$$-(1 - \gamma) \frac{e}{\gamma m_\mu} \vec{B}$$

Cyclotron frequency for momentum vector rotation



$$\vec{\omega}_c = \frac{e}{\gamma m_\mu} \vec{B}$$

Relativistic Correction

Fermilab Muon g-2 Experiment



USA

- Boston
- Cornell
- Illinois
- James Madison
- Kentucky
- Massachusetts
- Michigan
- Michigan State
- Mississippi
- North Central
- Northern Illinois
- Regis
- Virginia
- Washington

USA National Labs

- Argonne
- Brookhaven
- Fermilab

181 collaborators
33 Institutions
7 countries



China

- Shanghai Jiao Tong



Germany

- Dresden
- Mainz



Italy

- Frascati
- Molise
- Naples
- Pisa
- Roma Tor Vergata
- Trieste
- Udine



Korea

- CAPP/IBS
- KAIST



Russia

- Budker/Novosibirsk
- JINR Dubna



United Kingdom

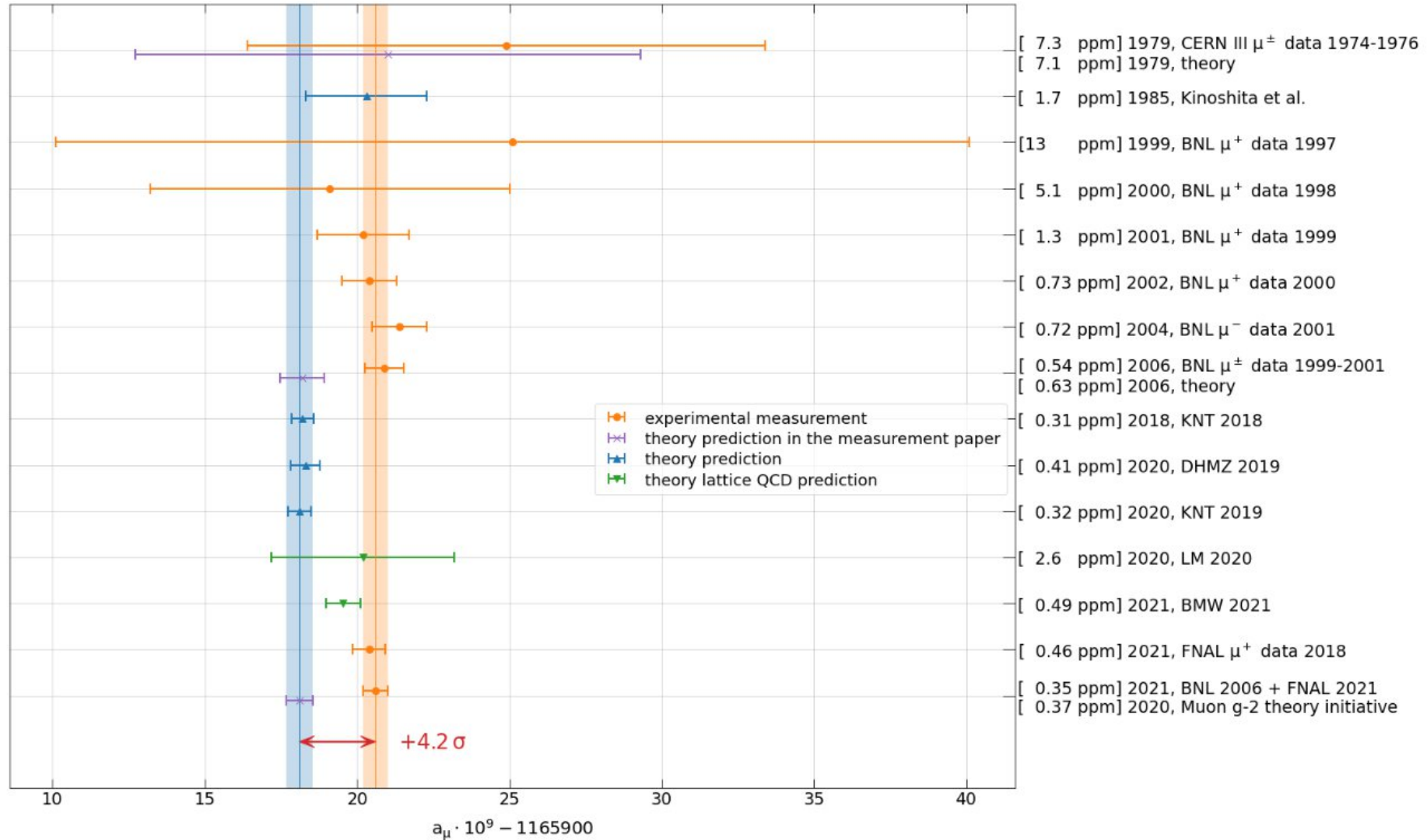
- Lancaster/Cockcroft
- Liverpool
- Manchester
- University College London



Muon g-2 Collaboration Meeting @ Elba, May 2019

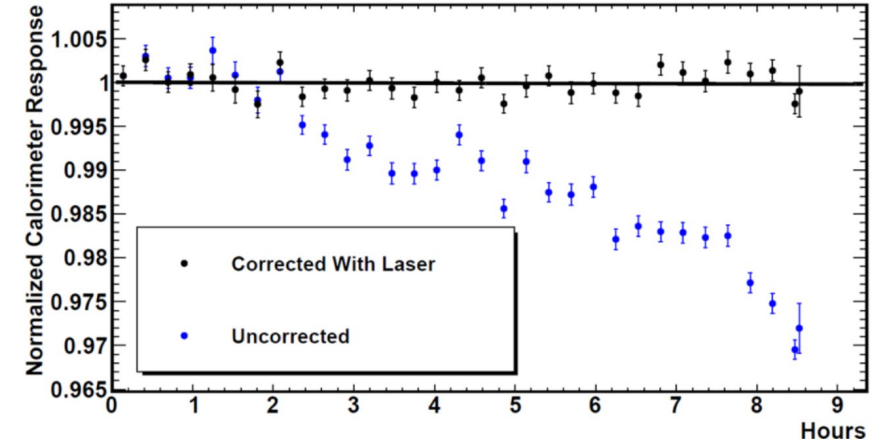
History of Muon Anomaly

History of muon anomaly measurements and predictions

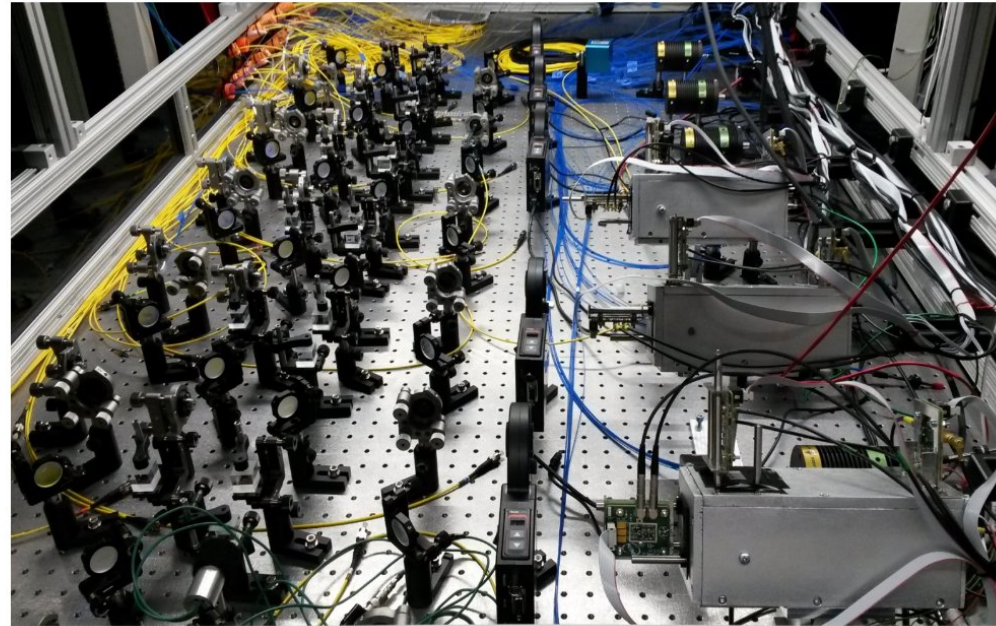
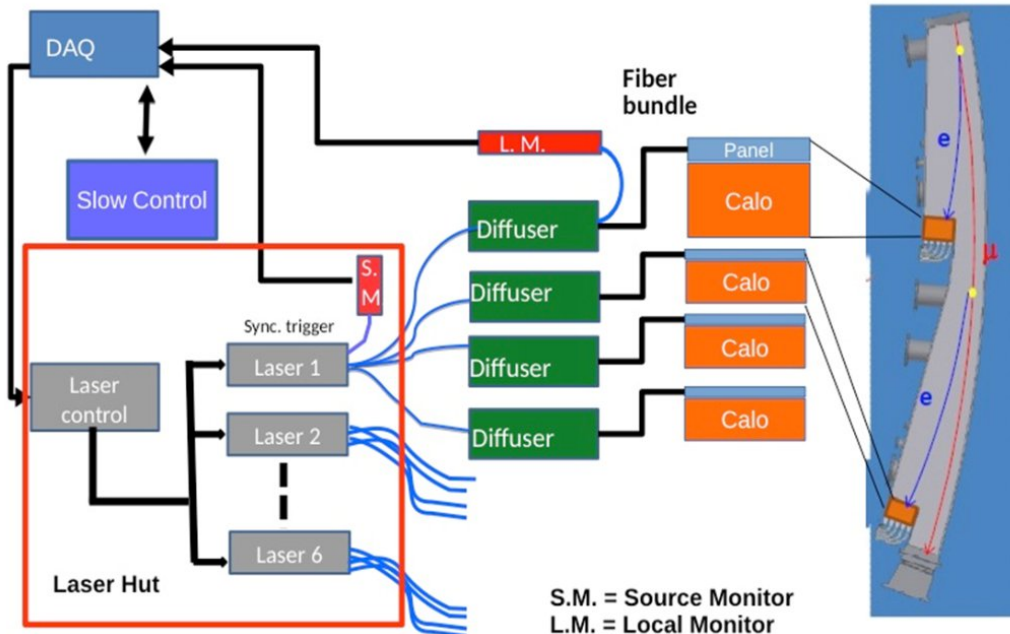


Laser Calibration

- Sends laser pulse synchronously on all calorimeter channels:
 - provide calibration for the SiPMs response,
 - short and long term calibration of the SiPM gain function,
 - troubleshoot calorimeter and DAQ systems,
 - additional synchronization signals.



Stable gain 10^{-4} achieved

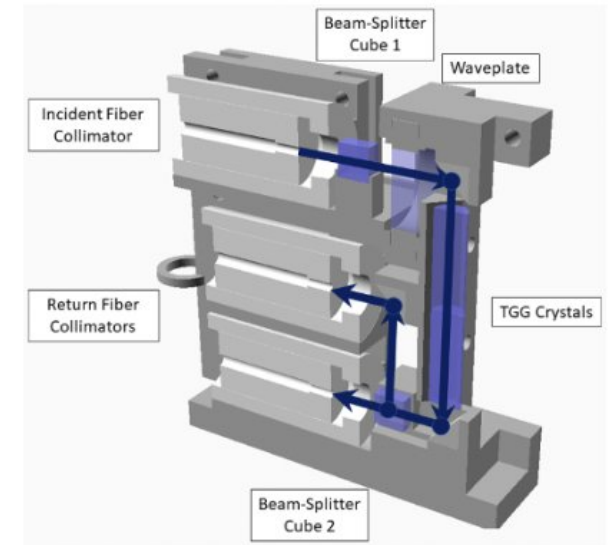


Run-2/3 Uncertainty Improvement

- Hardware Improvement:
 - Replacement of damaged ESQ resistors:
 - Less beam motion (vertical width) in the measurement, improving C_{pa} correction and uncertainty.
 - Hall/Ring temperature stabilized:
 - The storage ring magnet shape is insensitive to the temperature fluctuation, less prone to changes in beam behavior via the changes in magnetic field.
 - less changes to the detector gain.
 - Kicker strength improved:
 - No underkick relative to its ideal orbit, reduce oscillation around the center of the storage region.

Run-2/3 Uncertainty Improvement

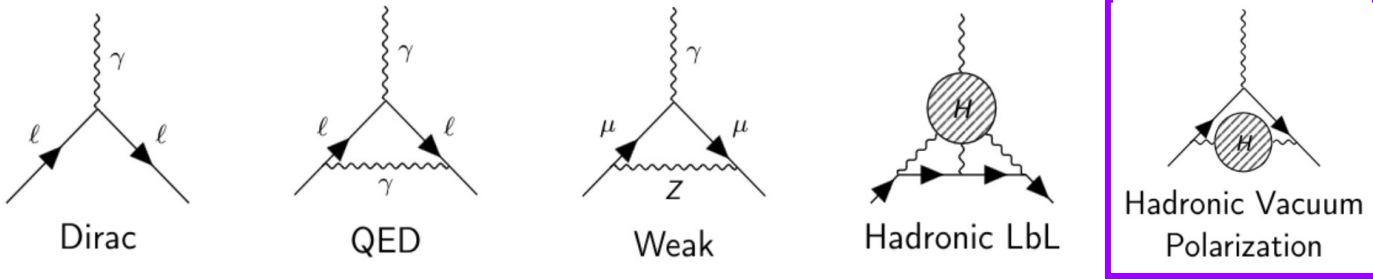
- Analysis Improvement:
 - Field Transient Measurement:
 - Complete Quad transient field measurement around the ring.
 - Improved kicker transient field measurement with fiber magnetometer.
 - Analysis technique improvement:
 - New positron reconstruction algorithms.
 - Improved pile-up subtraction technique.



Run-2/3 Systematic

Quantity	Correction [ppb]	Uncertainty [ppb]	
ω_a^m (statistical)	–	434	201
ω_a^m (systematic)	–	56	25
C_e	451	53	32
C_p	170	13	10
C_{pa}	-27	75	13
C_{dd}	-15	-	17
C_{ml}	0	5	3
$f_{\text{calib}} \langle \omega_p'(\vec{r}) \times M(\vec{r}) \rangle$	–	56	46
B_k	-21	37	13
B_q	-21	92	20
$\mu_p'(34.7^\circ)/\mu_e$	–	10	11
m_μ/m_e	–	22	22
$g_e/2$	–	0	0
Total systematic	–	157	70
Total external parameters	–	25	25
Totals	622	462	215

Standard Model Prediction of a_μ

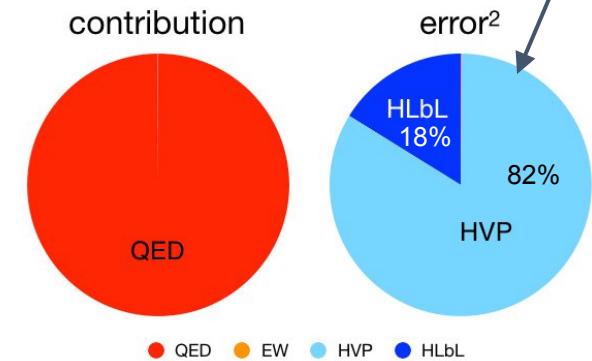
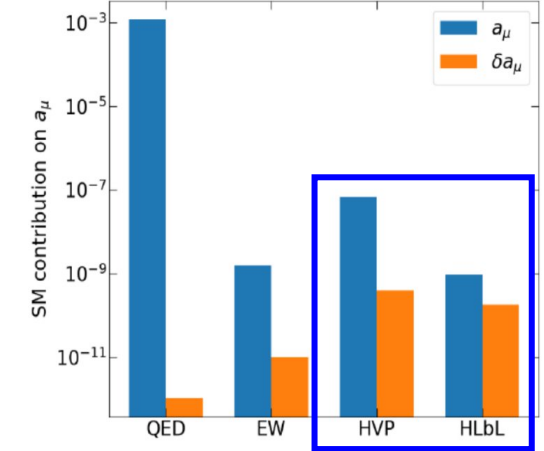


$$a_\mu^{SM} = 0 + a_\mu^{QED} + a_\mu^{Weak} + a_\mu^{HLbL} + a_\mu^{HVP}$$

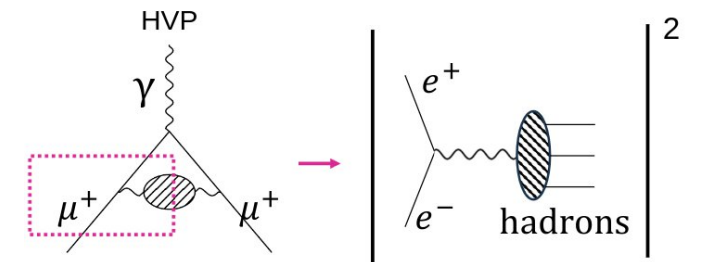
$$a_\mu^{SM} = 116591810(43) \times 10^{-11} \quad (0.37 \text{ ppm})$$

[Phys. Rep. 887, 1 \(2020\)](#)

- QED is the dominant processes contributing to the interaction.
- EW contribution is suppressed by $(m_\mu/M_W)^2$.
- Non-perturbative terms, HLbL, **HVP**, are calculated with:
 - Lattice-QCD (ab initio, via numerical simulations in Euclidean spacetime.)
 - data-driven dispersive relation (input data from experiment)
- The prediction's uncertainty is dominated by **HVP**'s term.



HVP calculation with $ee \rightarrow$ hadrons data



References

- T. Aoyama, N. Asmussen, M. Benayoun, J. Bijnens, T. Blum et al. The anomalous magnetic moment of the muon in the standard model, [Phys. Rep. 887, 1 \(2020\)](#).
- G. W. Bennett et al. (Muon g-2 Collaboration), Final measurement at BNL, [Phys. Rev. D 73, 072003 \(2006\)](#).
- Borsanyi, S., Fodor, Z., Guenther, J.N. et al. Leading hadronic contribution to the muon magnetic moment from lattice QCD. [Nature 593, 51–55 \(2021\)](#)
- D. P. Aguillard et al. (Muon g-2 Collaboration), Measurement of the Positive Muon Anomalous Magnetic Moment to 0.20 ppm. [Phys. Rev. Lett. 131, 161802](#)
- D. Hanneke, S. Fogwell Hoogerheide, and G. Gabrielse. Cavity control of a single-electron quantum cyclotron: Measuring the electron magnetic moment. [Phys. Rev. A 83, 052122](#)
- Peter J. Mohr, Barry N. Taylor, and David B. Newell. CODATA recommended values of the fundamental physical constants: 2010. [Rev. Mod. Phys. 84, 1527](#)
- W. Liu et al. High precision measurements of the ground state hyperfine structure interval of muonium and of the muon magnetic moment. [Phys. Rev. Lett. 82, 711](#)